A two-pressure model for slightly compressible single phase flow in bi-structured porous media

Cyprien Soulaine, Yohan Davit, Michel Quintard

A two-pressure model for slightly compressible single phase flow in bi-structured porous media

Cyprien Soulaine [a,*], Yohan Davit [a,b,c], Michel Quintard [a,b]

[a] Université de Toulouse; INPT, UPS; IMFT (Institut de Mécanique des Fluides de Toulouse); Allée Camille Soula, F-31400 Toulouse, France
[b] CNRS; IMFT; F-31400 Toulouse, France
[c] University of Oxford, Mathematical Institute, 24-29 St. Giles', Oxford, OX1 3LB, United Kingdom

HIGHLIGHTS

- Upscaling of slightly compressible single phase flow in bi-structured porous media.
- The resulting macroscopic system is a two-pressure equations.
- All the effective coefficients are entirely determined by three closure problems.
- Comparison with pore-scale direct numerical simulations for a particle filter.

Keywords:
Porous media
Volume averaging
Upscaling
Slightly compressible flow
Bi-structured

ABSTRACT

Problems involving flow in porous media are ubiquitous in many natural and engineered systems. Mathematical modeling of such systems often relies on homogenization of pore-scale equations and macroscale continuum descriptions. For single phase flow, Stokes equations at the pore-scale are generally approximated by Darcy's law at a larger scale. In this work, we develop an alternative model to Darcy's law that can be used to describe slightly compressible single phase flow within bi-structured porous media. We use the method of volume averaging to upscale mass and momentum balance equations with the fluid phase split into two fictitious domains. The resulting macroscale model combines two coupled equations for average pressures with *regional* Darcy's laws for velocities. Contrary to classical dual-media models, the averaging process is applied directly to Stokes problem and not to Darcy's laws. In these equations, effective parameters are expressed via integrals of mapping variables that solve boundary value problems over a representative unit cell. Finally, we illustrate the behavior of these equations for model porous media and validate our approach by comparing solutions of the homogenized equations with computations of the exact microscale problem.

1. Introduction

Porous media are intrinsically highly complex materials, with the consequence that transport phenomena generally occur over a broad spectrum of spatial and temporal scales. Even for single phase flow, this variety of characteristic time and length scales may preclude the use of a one-equation continuum representation. For instance, advection and diffusion of a single species in a system with stagnant zones or dead-end pores are better represented macroscopically by a two-equation model in which the species concentration is divided into mobile and immobile fractions (see Coats and Smith, 1964 for an early discussion on the subject). In many applications (including flow in fractured media, automobile soot filters or chemical and biochemical reactors), the porous medium itself exhibits a distinct two-region topology, e.g., as a consequence of a contrast of porosity or a difference in the pore structure geometry. Herein, we will use the term bi-structured to describe these porous media, a term which represents a more general definition than the traditional dual-media or dual-porosity terminology. With this definition, one may differentiate each region according to a number of different properties including the topology of the fluid flow. For example, in fractured media, fractures represent a zone of preferential flow whereas the amplitude of the velocity field in the matrix blocks is often orders of magnitude smaller. In the literature, solute transport in such systems is often described using mobile/immobile models. Rapid advective transport in the mobile domain is accompanied by diffusive mass transfer of the solute in the immobile domains. This contrast of time scales may strongly impact the concentration field and it is well known that breakthrough curves, in such configurations, typically exhibit strong tailing effects.

* Corresponding author. Tel.: +33 5 34 32 28 75.
E-mail address: cyprien.soulaine@imft.fr (C. Soulaine).

http://dx.doi.org/10.1016/j.ces.2013.03.060

More generally, if time and length scales characterizing the two regions differ significantly, non-equilibrium models may be mandatory. An example of one such model is a generic two-equation formulation (see Coats and Smith, 1964; Brusseau and Rao, 1990) in which average concentrations are defined over each region separately. In this model, each equation involves the average velocity within each region; velocity fields that are also known as "regional velocities". The situation simplifies for mobile/immobile systems since the regional velocity of one region is negligible and, therefore, the net superficial velocity corresponds to the superficial velocity of the mobile region. However, bi-structured systems are not necessarily of the mobile/immobile type. If advection cannot be neglected in the slower region, a mobile/mobile model (Skopp et al., 1981; Gerke and VanGenuchten, 1993; Ahmadi et al., 1998; Cherblanc et al., 2003) with two different regional velocities may be necessary. In practice, experimental measurements of these regional velocities are difficult and one can often access only the total imposed filtration velocity. Regional velocities may therefore be determined indirectly by inverse optimization techniques, although such approaches will be primarily useful in large-scale 1D cases. For interpreting a complete 3D macroscale problem, the momentum transport equations are needed along with mass transport equations. This issue has been addressed theoretically in Quintard and Whitaker (1996) using the volume averaging technique. In this cited paper, large-scale momentum transport equations are determined via a two-step upscaling procedure: Stokes equations are first averaged to obtain a Darcy-scale description within each region and, then, a regional averaging is performed in order to obtain the large-scale equations. This was done in Quintard and Whitaker (1996) for the flow of a slightly compressible fluid and led to a large-scale two-equation model involving two average pressures; a result thus generalizing the classical two-equation model of Barenblatt et al. (1960). Further, average velocities can be determined via regional Darcy's laws in which regional permeability tensors are expressed as integrals of mapping variables that solve the so-called closure problems defined at the Darcy-scale (see Quintard and Whitaker, 1998 and Fig. 1). Again, this derivation is a recursive procedure based on a successive averaging from the pore-scale to the Darcy-scale and then to the large-scale. Typically, the following constraints must be satisfied:

1. The pore-scale characteristic length must be much smaller than the characteristic lengths of the two regions (separation of scales), so that Stokes can be upscaled to Darcy's law within each region.
2. The subsequent upscaling from Darcy's law within each region to a large-scale Darcy's law or a dual-media model (as developed in Quintard and Whitaker, 1996) also requires a separation of scales between the regional and large-scale characteristic lengths.

Therefore, this two-region approach applies only to large systems and cannot be used directly for some bi-structured porous media at the pore-scale, for which the first separation of scales does not hold. In this work, our goal is to derive one such two-pressure model *directly* from the Stokes problem at the pore-scale.

There are many industrial applications involving bi-structured porous media where it may be useful to split the flow of a single phase into two coupled continuum equations. This is the case, for instance, in tangential filters in which two sets of channels are exchanging via small holes or porous walls (Belfort et al., 1994; Zeman and Zydney, 1996; Oxarango et al., 2004; Borsi and Lorain, 2012). Recently, in an attempt to model the liquid distribution within structured packings used in chemical engineering processes, Mahr and Mewes (2008) have found convenient to split the (physically homogeneous) liquid phase into two fictitious phases. This approach was motivated by the fact that the structured packings are made of an assembly of corrugated sheets where two-adjacent sheets are inclined by a given angle with respect to the vertical axis and the opposite of this angle, respectively. As a consequence, the liquid phase behaves as if split into two pseudo-phases flowing along each sheet with a preferential direction. These phases are not (except perhaps at very low saturation) completely independent since adjacent sheets are in contact and the wetting liquid can flow from one sheet to the other. In the paper referenced above, this transfer between the two liquid phases is treated using a heuristic function involving the difference between the volume fraction of fluid in each phase. Although

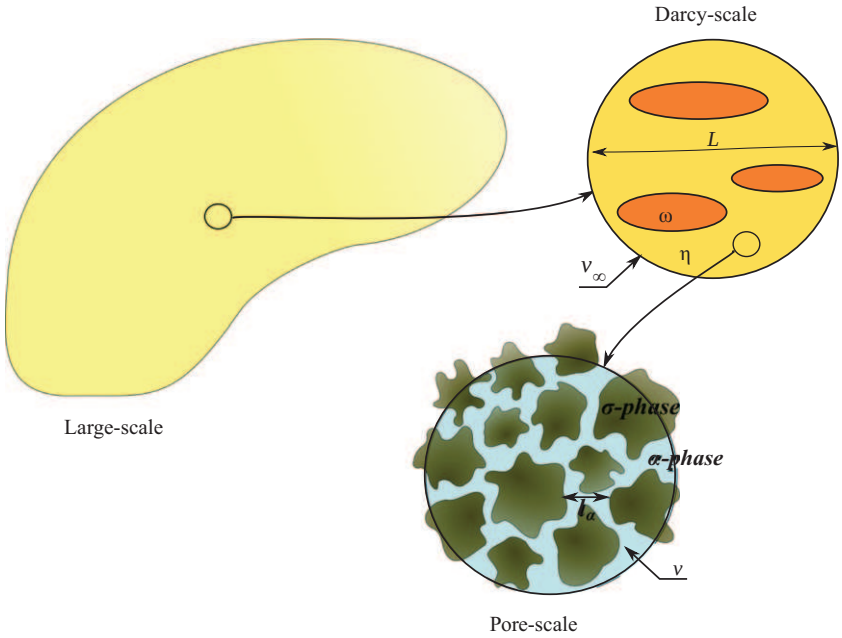

Fig. 1. Schematic representation of the hierarchy of length scales of a classical dual-porous medium as presented in Quintard and Whitaker (1996).

theoretical arguments based on a volume averaging theory are discussed by the authors, the developments are at some point heuristic and we believe that a complete theoretical derivation of the macroscale models is still necessary. For simplicity, we will focus in this paper on the fully saturated case.

The paper is organized as follows. In Section 2, we present the equations that govern the fluid motion through a bi-structured porous medium. The flow of the single phase is divided into two fictitious phases defined by the topology of the problem. In Section 3, we derive Darcy's law as a pedagogical exercise that facilitates later comparison with the two-pressure model. In Section 4, we present theoretical developments for the derivation of the two-pressure model with phase splitting. In Section 5, we solve numerically the flow through a simplified particulate filter using Darcy's law and the two-pressure model. The macroscale models are then compared with direct numerical simulations of the pore-scale problem in the absence of adjustable parameters. Then, in Section 6, we investigate the potential importance of the coupling cross-terms that appear in the macroscale model, by simulating flow through a dual porous medium.

2. Preliminaries

In this section, we present the pore-scale mass and momentum transport equations, the two-phase splitting methodology and several preliminary results concerning the averaging method.

2.1. Pore-scale problem

Herein, we will use the index α to denote the fluid phase (domain V_α) and σ to denote the solid phase. The mass balance equation in the fluid phase can be expressed as the following partial differential equation:

$$\frac{\partial \rho_\alpha}{\partial t} + \nabla\cdot(\rho_\alpha \mathbf{v}_\alpha) = 0 \quad \text{in } V_\alpha, \tag{1}$$

where ρ_α is the density in the $\alpha-$phase and $\mathbf{v}_\alpha$ is the velocity field. Further, we will focus on creeping conditions, so that the momentum balance equation simplifies to the following Stokes equation:

$$0 = -\nabla p_\alpha + \rho_\alpha \mathbf{g} + \mu \nabla^2 \mathbf{v}_\alpha \quad \text{in } V_\alpha, \tag{2}$$

where p_α is the pressure, $\mathbf{g}$ is the gravitational acceleration and μ is the dynamic viscosity. At the fluid–solid interface, $\mathcal{A}_{\alpha\sigma}$, we impose the no-slip boundary condition

$$\mathbf{v}_\alpha = 0 \quad \text{at } \mathcal{A}_{\alpha\sigma}. \tag{3}$$

2.2. Phase splitting

As discussed in the Introduction of this paper, we are interested in bi-structured porous media that typically exhibit a bi-modal distribution of one of the flow properties, e.g., the amplitude or direction of the velocity field, as illustrated in Fig. 2. This topology suggests that splitting the phase (α) into two fictitious domains (γ) and (β) may be a useful operation. Further, we will consider that these regions are static and can be defined arbitrarily (although there is probably an optimal way to split the domain). In fact, the most pertinent delineation will strongly depend on the problem of interest and the purpose of the model. Applications to mass transfer through dual-porosity structures may require criteria based on the magnitude of the velocity or the Péclet number. For example, we could split the regions by using a number of image processing algorithms on the velocity magnitude spectrum and facilitate the identification of, say, a mobile and an immobile regions. In the case of the structured packing that was mentioned in the Introduction, the splitting could be performed using the orientation spectrum of the velocity field, i.e., the orientation of the corrugated sheets (Mahr and Mewes, 2008; Soulaine, 2012)

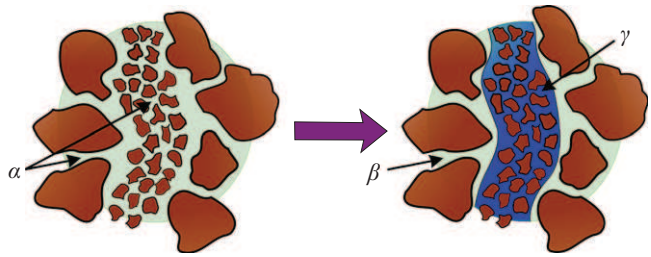

Fig. 2. Schematic representation of a model bi-structured porous medium. In this example, the average amplitude of the flow within the $\gamma-$region is significantly larger than the average amplitude of the flow within the $\beta-$region. Therefore, the $\alpha-$phase may be split into two fictitious phases, β and γ, for upscaling purposes.

Eq. (1) yields

$$\frac{\partial \rho_i}{\partial t} + \nabla\cdot(\rho_i \mathbf{v}_i) = 0 \quad \text{in } V_i \quad \text{with } i = \beta \quad \text{or} \quad \gamma. \tag{4}$$

Similarly, Stokes equation may be written as

$$0 = -\nabla p_i + \rho_i \mathbf{g} + \mu \nabla^2 \mathbf{v}_i \quad \text{in } V_i, \quad i = \beta \quad \text{or} \quad \gamma. \tag{5}$$

Since we are considering the same fluid within phases (γ) and (β), we have identical physical properties on both sides of the boundary $\mathcal{A}_{\beta\gamma}$. For instance, we have considered that the viscosity, μ, is constant and the density obeys the same thermodynamical laws in phases (γ) and (β) (see details in Section 2.4 in the case of a slightly compressible fluid).

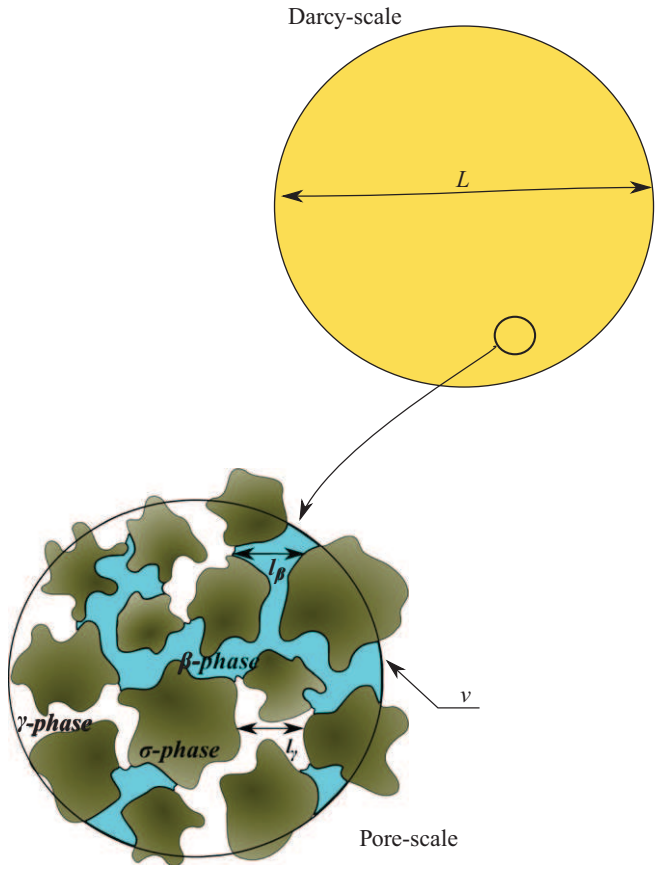

Fig. 3. Schematic representation of the hierarchy of length scales of a model porous medium and of a typical representative volume.

The no-slip boundary condition on the fluid/solid surface area, $\mathcal{A}_{i\sigma}$, supplies

$$\mathbf{v}_i = 0 \quad \texttt{at } \mathcal{A}_{i\sigma}, \quad i = \beta \quad \text{or} \quad \gamma. \tag{6}$$

On the interface between the two fluid phases, $\mathcal{A}_{\beta\gamma}$, we will use continuity conditions for the velocity and pressures

$$\mathbf{v}_\beta = \mathbf{v}_\gamma \quad \texttt{at } \mathcal{A}_{\beta\gamma}, \tag{7}$$

and

$$p_\beta = p_\gamma \quad \texttt{at } \mathcal{A}_{\beta\gamma}, \tag{8}$$

as well as their derivatives.

A priori, the boundary conditions, Eqs. (7) and (8), suggest that a two-equation model with an exchange term based on averaged pressures and/or velocities differences may be adapted to the macroscale description of this system.

2.3. Definitions and theorems

In this section, we present the definitions and theorems that are needed to perform volume averaging. We will only give a brief outline of the technique and the reader is referred to Whitaker (1999) for a more detailed presentation.

The multiscale problem under consideration is schematically represented in Fig. 3. This figure illustrates the three characteristic length-scales that are involved in this system: (1) the macroscale, L; (2) the radius, R, of the averaging volume, $\mathcal{V}$; and (3) the average pore size for region α, ℓ_α (where $\alpha = \beta, \gamma$). Throughout this paper, we use the following separation of scales assumption: $\ell_\alpha \ll R \ll L$. We have discussed differences with the work in Quintard and Whitaker (1996) in the Introduction of this paper and illustrated the different scales in Figs. 3 and 1.

For a tensor ψ_i (order 0, 1 or 2) defined in the i-phase, we will use the average notation

$$\langle \psi_i \rangle = \frac{1}{V} \int_{V_i} \psi_i \, dV, \tag{9}$$

and the corresponding *intrinsic* average

$$\langle \psi_i \rangle^i = \frac{1}{V_i} \int_{V_i} \psi_i \, dV. \tag{10}$$

These two expressions are connected by

$$\langle \psi_i \rangle = \varepsilon_i \langle \psi_i \rangle^i \quad \text{with } \varepsilon_i = \frac{V_i}{V}, \tag{11}$$

where V_i is the volume of the i-phase and ε_i is the volume fraction of the i-phase. Throughout this paper, the porous medium is homogeneous and ε_i is constant.

To perform the perturbation analysis, we will use Gray's decomposition (see in Gray, 1975)

$$\psi_i = \langle \psi_i \rangle^i + \tilde{\psi}_i, \tag{12}$$

and we will impose the following separation of length scales, $\ell \ll R \ll L$, which yields (see in Whitaker, 1999):

$$\langle \tilde{\psi}_i \rangle = 0. \tag{13}$$

To interchange integrals and derivatives, we will use the following theorems. For spatial averaging, we have

$$\langle \nabla \psi_i \rangle = \nabla \langle \psi_i \rangle + \frac{1}{V} \int_{\mathcal{A}_i} \mathbf{n}_i \psi_i \, dA, \tag{14}$$

and a similar expression for the divergence of a tensor field $\mathbf{A}_i$ (order 1 or 2)

$$\langle \nabla \cdot \mathbf{A}_i \rangle = \nabla \cdot \langle \mathbf{A}_i \rangle + \frac{1}{V} \int_{\mathcal{A}_i} \mathbf{n}_i \cdot \mathbf{A}_i \, dA. \tag{15}$$

In these theorems, $\mathcal{A}_i$ denotes all the interfaces in contact with the i-phase and $\mathbf{n}_i$ is the outwards normal vector. On averaging over the phase (α), this theorem reads

$$\langle \nabla \psi_\alpha \rangle = \nabla \langle \psi_\alpha \rangle + \frac{1}{V} \int_{\mathcal{A}_{\alpha\sigma}} \mathbf{n}_{\alpha\sigma} \psi_\alpha \, dA. \tag{16}$$

On averaging over the phases (β) or (γ), the interface $\mathcal{A}_i$ contains both the fluid/solid and fluid/fluid interfaces. Consequently, Eq. (14) may be written as

$$\langle \nabla \psi_\beta \rangle = \nabla \langle \psi_\beta \rangle + \frac{1}{V} \int_{\mathcal{A}_{\beta\sigma}} \mathbf{n}_{\beta\sigma} \psi_\beta \, dA + \frac{1}{V} \int_{\mathcal{A}_{\beta\gamma}} \mathbf{n}_{\beta\gamma} \psi_\beta \, dA. \tag{17}$$

Finally, we will use the following simplifications. We will consider that the volume fractions are constant, so that

$$\nabla \varepsilon_i = -\frac{1}{V} \int_{\mathcal{A}_i} \mathbf{n}_i \, dA = 0, \tag{18}$$

and that the interfaces are static, so that

$$\left\langle \frac{\partial \psi_i}{\partial t} \right\rangle = \frac{\partial \langle \psi_i \rangle}{\partial t}. \tag{19}$$

2.4. Slightly compressible approximation and thermodynamics

Throughout this paper, we will work under isothermal conditions so that the pressure completely defines the thermodynamical state of the system. We will consider that the fluid density can be written as a function of the pressure

$$\rho_\alpha = F(p_\alpha). \tag{20}$$

Further, on injecting Eq. (12) into Eq. (20) and assuming that perturbations remain small enough to perform a zeroth-order approximation, we obtain the following macroscale relationship (see Whitaker, 1987; Quintard and Whitaker, 1996):

$$\langle \rho_\alpha \rangle^\alpha = F(\langle p_\alpha \rangle^\alpha). \tag{21}$$

In this work, we consider the following approximation as presented in Quintard and Whitaker (1996):

$$\langle \rho_\alpha \rangle^\alpha \simeq \rho^0 [1 + c(\langle p_\alpha \rangle^\alpha - p^0)], \tag{22}$$

where p^0 is a reference pressure; ρ^0 is the corresponding reference density; and c is a compressibility coefficient given by

$$c = \frac{1}{\rho^0} \left(\frac{\partial F}{\partial p} \right)_{p = p^0} \quad \texttt{with } \rho^0 = F(p^0). \tag{23}$$

Following Quintard and Whitaker (1996), we simplify notations using hydrostatic pressures

$$P_\alpha = p_\alpha - p^0 - \rho^0 \mathbf{g} \cdot \mathbf{r}_\alpha, \tag{24}$$

where $\mathbf{r}_\alpha$ is the position vector. With these definitions, we remark that

$$\langle P_\beta \rangle^\beta - \langle P_\gamma \rangle^\gamma = \langle p_\beta \rangle^\beta - \langle p_\gamma \rangle^\gamma. \tag{25}$$

Further, as shown in Quintard and Whitaker (1996) for disordered porous media, we have

$$\nabla \langle P_\alpha \rangle^\alpha = \nabla \langle p_\alpha \rangle^\alpha - \rho^0 \mathbf{g}. \tag{26}$$

On using Eq. (22) into Eq. (26), we obtain

$$\nabla \langle P_\alpha \rangle^\alpha = \nabla \langle p_\alpha \rangle^\alpha - \langle \rho_\alpha \rangle^\alpha \mathbf{g} + \rho^0 c (\langle p_\alpha \rangle^\alpha - p^0) \mathbf{g}. \tag{27}$$

We further simplify these equations by limiting our study to slightly compressible fluids, defined here by the following inequalities:

$$c(\langle p_\alpha \rangle^\alpha - p^0) \ll 1 \quad \texttt{and} \quad \rho^0 c (\langle p_\alpha \rangle^\alpha - p^0) g \ll \| \nabla \langle P_\alpha \rangle^\alpha \|. \tag{28}$$

Consequently, we will approximate Eq. (26) using

$$\nabla\langle P_\alpha\rangle^\alpha \approx \nabla\langle p_\alpha\rangle^\alpha - \langle\rho_\alpha\rangle^\alpha \mathbf{g}. \tag{29}$$

Following a similar approach, the evolution rates can also be approximated as

$$\frac{\partial\langle\rho_\alpha\rangle^\alpha}{\partial t} = c\rho^0 \frac{\partial\langle p_\alpha\rangle^\alpha}{\partial t} = c\rho^0 \frac{\partial\langle P_\alpha\rangle^\alpha}{\partial t}. \tag{30}$$

3. One-pressure model (Darcy's law)

In this section, we will briefly present results obtained in Whitaker (1986b) which led to the derivation of the one-pressure model, i.e., Darcy's law. This will facilitate the comparison between Darcy's law and the two-pressure model developed in the next section.

3.1. Volume averaging

To obtain the macroscale equations, we average Eqs. (1) and (2). For the mass balance equation, it yields

$$\frac{\partial\langle\rho_\alpha\rangle}{\partial t} + \nabla\cdot\langle\rho_\alpha\mathbf{v}_\alpha\rangle = 0. \tag{31}$$

Stokes equation becomes

$$0 = -\nabla\langle p_\alpha\rangle + \langle\rho_\alpha\rangle\mathbf{g} + \mu\nabla^2\langle\mathbf{v}_\alpha\rangle + \mu\nabla\cdot\left(\frac{1}{V}\int_{\mathcal{A}_\alpha}\mathbf{n}_\alpha\mathbf{v}_\alpha\, d\mathcal{A}\right) + \frac{1}{V}\int_{A_{\alpha\sigma}}\mathbf{n}_{\alpha\sigma}\cdot(-p_\alpha\mathbf{I} + \mu\nabla\mathbf{v}_\alpha)\, dA. \tag{32}$$

To facilitate solution, we combine the perturbation decomposition, Eq. (12), the average relations, Eq. (11), the scale constraints, $\ell \ll R \ll L$, and the thermodynamical relationships, to obtain the following two equations (for further details, see in Whitaker, 1986b):

$$\frac{\partial\varepsilon_\alpha\langle\rho_\alpha\rangle^\alpha}{\partial t} + \nabla\cdot(\varepsilon_\alpha\langle\rho_\alpha\rangle^\alpha\langle\mathbf{v}_\alpha\rangle^\alpha) + \nabla\cdot\langle\tilde{\rho}_\alpha\tilde{\mathbf{v}}_\alpha\rangle = 0, \tag{33}$$

and

$$0 = -\nabla\langle p_\alpha\rangle^\alpha + \langle\rho_\alpha\rangle^\alpha\mathbf{g} + \mu\nabla^2\langle\mathbf{v}_\alpha\rangle^\alpha + \frac{\varepsilon_\alpha^{-1}}{V}\int_{\mathcal{A}_{\alpha\sigma}}\mathbf{n}_{\alpha\sigma}\cdot(-\tilde{p}_\alpha\mathbf{I} + \mu\nabla\tilde{\mathbf{v}}_\alpha)\, dA. \tag{34}$$

In addition, we will assume that deviations of the density are relatively small, $\tilde{\rho}_\alpha \ll \langle\rho_\alpha\rangle^\alpha$, and that Brinkman's term, $\mu\nabla^2\langle\mathbf{v}_\alpha\rangle^\alpha$, can be neglected. These assumptions supply

$$\varepsilon_\alpha\frac{\partial\langle\rho_\alpha\rangle^\alpha}{\partial t} + \nabla\cdot(\langle\rho_\alpha\rangle^\alpha\langle\mathbf{v}_\alpha\rangle) = 0, \tag{35}$$

and

$$0 = -\nabla\langle p_\alpha\rangle^\alpha + \langle\rho_\alpha\rangle^\alpha\mathbf{g} + \frac{\varepsilon_\alpha^{-1}}{V}\int_{\mathcal{A}_{\alpha\sigma}}\mathbf{n}_{\alpha\sigma}\cdot(-\tilde{p}_\alpha\mathbf{I} + \mu\nabla\tilde{\mathbf{v}}_\alpha)\, dA. \tag{36}$$

3.2. Deviations

Rearranging Eq. (12) in the form $\tilde{\psi}_i = \psi_i - \langle\psi_i\rangle^i$ suggests that the initial boundary value problem that describes the behavior of the perturbations can be obtained by subtracting Eqs. (33) and (34) from Eqs. (1) and (2), respectively. On assuming quasi-stationarity of $\tilde{\rho}_\alpha$ and imposing $\tilde{\rho}_\alpha \ll \langle\rho_\alpha\rangle^\alpha$, the continuity equation yields

$$\nabla\cdot\tilde{\mathbf{v}}_\alpha = 0 \quad \text{in } V_\alpha, \tag{37}$$

and the original Stokes problem may be written as

$$0 = -\nabla\tilde{p}_\alpha + \mu\nabla^2\tilde{\mathbf{v}}_\alpha - \frac{\varepsilon_\alpha^{-1}}{V}\int_{\mathcal{A}_{\alpha\sigma}}\mathbf{n}_\alpha\cdot(-\tilde{p}_\alpha\mathbf{I} + \mu\nabla\tilde{\mathbf{v}}_\alpha)\, dA \quad \text{in } V_\alpha, \tag{38}$$

with the no-slip boundary condition giving

$$\tilde{\mathbf{v}}_\alpha = -\langle\mathbf{v}_\alpha\rangle^\alpha \quad \text{at } \mathcal{A}_{\alpha\sigma}. \tag{39}$$

Given the linearity of the above spatial operators, we can decompose the deviation fields for the velocity and pressure as

$$\tilde{\mathbf{v}}_\alpha = \mathbf{A}_\alpha\cdot\langle\mathbf{v}_\alpha\rangle^\alpha, \tag{40}$$

$$\tilde{p}_\alpha = \mu\mathbf{a}_\alpha\cdot\langle\mathbf{v}_\alpha\rangle^\alpha. \tag{41}$$

We will refer to the tensor fields $\mathbf{A}_\alpha$ and $\mathbf{a}_\alpha$ as closure parameters or mapping tensors. Substituting Eqs. (40) and (41) into Eqs. (37) and (38), we obtain the following boundary value problem:

$$\nabla\cdot\mathbf{A}_\alpha = 0 \quad \text{in } V_\alpha, \tag{42}$$

$$0 = -\nabla\mathbf{a}_\alpha + \nabla^2\mathbf{A}_\alpha + \varepsilon_\alpha\mathbf{K}_\alpha^{-1} \quad \text{in } V_\alpha, \tag{43}$$

$$\mathbf{A}_\alpha = -\mathbf{I} \quad \text{at } \mathcal{A}_{\alpha\sigma}, \tag{44}$$

where we have used the definition

$$\varepsilon_\alpha\mathbf{K}_\alpha^{-1} = -\frac{\varepsilon_\alpha^{-1}}{V}\int_{\mathcal{A}_{\alpha\sigma}}\mathbf{n}_\alpha\cdot(-\mathbf{I}\mathbf{a}_\alpha + \nabla\mathbf{A}_\alpha)\, dA. \tag{45}$$

We will assume that the porous medium structure can be represented locally by a periodic geometry

$$\mathbf{A}_\alpha(\mathbf{r} + \mathbf{l}_k) = \mathbf{A}_\alpha(\mathbf{r}) \quad \text{and} \quad \mathbf{a}_\alpha(\mathbf{r} + \mathbf{l}_k) = \mathbf{a}_\alpha(\mathbf{r}) \quad \text{with } k = 1,2,3. \tag{46}$$

In addition we impose zero-average constraints

$$\langle\mathbf{A}_\alpha\rangle = 0 \quad \text{and} \quad \langle\mathbf{a}_\alpha^0\rangle = 0, \tag{47}$$

to ensure that the average of deviations is zero.

For computational purposes, this integro-differential formulation can be simplified to develop a purely differential form where $\mathbf{K}_\alpha^{-1}$ disappears. The developments are given in Appendix A.

3.3. Macroscale equations

Using Eqs. (40) and (41) into Eq. (36) yields

$$0 = -\nabla\langle p_\alpha\rangle^\alpha + \langle\rho_\alpha\rangle^\alpha\mathbf{g} - \mu\varepsilon_\alpha\mathbf{K}_\alpha^{-1}\cdot\langle\mathbf{v}_\alpha\rangle^\alpha, \tag{48}$$

which can be rearranged to form Darcy's law

$$\langle\mathbf{v}_\alpha\rangle = -\frac{\mathbf{K}_\alpha}{\mu}\cdot(\nabla\langle p_\alpha\rangle^\alpha - \langle\rho_\alpha\rangle^\alpha\mathbf{g}). \tag{49}$$

This may be written, with the hydrostatic pressure defined in Section 2.4, as

$$\langle\mathbf{v}_\alpha\rangle = -\frac{\mathbf{K}_\alpha}{\mu}\cdot\nabla\langle P_\alpha\rangle^\alpha. \tag{50}$$

We consider the thermodynamical constraint equation (28) and the relation equation (30), to obtain

$$\varepsilon_\alpha c\frac{\partial\langle P_\alpha\rangle^\alpha}{\partial t} + \nabla\cdot\langle\mathbf{v}_\alpha\rangle = 0. \tag{51}$$

Finally, combining Darcy's law with the continuity equation gives the following one-pressure equation:

$$\varepsilon_\alpha c\frac{\partial\langle P_\alpha\rangle^\alpha}{\partial t} = \nabla\cdot\left(\frac{\mathbf{K}_\alpha}{\mu}\cdot\nabla\langle P_\alpha\rangle^\alpha\right). \tag{52}$$

4. Two-pressure model

In this section, balance equations are averaged over each region separately (see Section 2.2). The upscaling technique itself is very similar to the one presented above for the derivation of Darcy's

law, except that our equations involve additional boundaries and source terms.

4.1. Volume averaging

Averaging Eq. (4) leads to the following macroscale equation

$$\frac{\partial\langle\rho_i\rangle}{\partial t}+\nabla\cdot\langle\rho_i\mathbf{v}_i\rangle+\frac{1}{V}\int_{\mathcal{A}_{\beta\gamma}}\mathbf{n}_{ij}\cdot\rho_i\mathbf{v}_i\,dA=0,\quad i\neq j, \tag{53}$$

where we have used the indices i and j to represent either the phase γ or β. In this equation, we have simplified the interface integral by using the no-slip boundary condition on $\mathcal{A}_{i\sigma}$. For the momentum balance equation, averaging Eq. (5) leads to (see Whitaker, 1986a, 1986b, 1994 for more details)

$$0=-\nabla\langle p_i\rangle^i+\langle\rho_i\rangle^i\mathbf{g}+\mu\nabla^2\langle\mathbf{v}_i\rangle^i+\frac{\varepsilon_i^{-1}}{V}\int_{\mathcal{A}_i}\mathbf{n}_i\cdot(-\tilde{p}_i\mathbf{I}+\mu\nabla\tilde{\mathbf{v}}_i)\,dA\quad\texttt{where } i=\beta,\gamma. \tag{54}$$

An important feature of this splitting operation is that both regions may exchange mass. This flux between the two regions is characterized by the quantity $\dot{m}$, which is defined by

$$\dot{m}=\frac{1}{V}\int_{\mathcal{A}_{\beta\gamma}}\mathbf{n}_{\beta\gamma}\cdot\rho_\beta\mathbf{v}_\beta\,dA=-\frac{1}{V}\int_{\mathcal{A}_{\beta\gamma}}\mathbf{n}_{\gamma\beta}\cdot\rho_\gamma\mathbf{v}_\gamma\,dA. \tag{55}$$

We can further expand this expression using the average-perturbation decomposition to obtain

$$\dot{m}=\frac{1}{V}\int_{\mathcal{A}_{\beta\gamma}}\mathbf{n}_{\beta\gamma}\cdot\tilde{\rho}_\beta\tilde{\mathbf{v}}_\beta\,dA+\frac{\langle\rho_\beta\rangle^\beta}{V}\int_{\mathcal{A}_{\beta\gamma}}\mathbf{n}_{\beta\gamma}\cdot\tilde{\mathbf{v}}_\beta\,dA+\left(\frac{1}{V}\int_{\mathcal{A}_{\beta\gamma}}\mathbf{n}_{\beta\gamma}\tilde{\rho}_\beta\,dA\right)\cdot\langle\mathbf{v}_\beta\rangle^\beta. \tag{56}$$

Formally, one should keep all terms involving $\tilde{\rho}_i$ and link these perturbations to average values during the closure process. However, similarly to what was done for Darcy's law, we will facilitate the analysis by imposing the order of magnitude slightly compressible constraint $\tilde{\rho}_i\ll\langle\rho_i\rangle^i$ and neglecting terms involving $\tilde{\rho}_i$. With these considerations, the mass exchange rate may be expressed as

$$\dot{m}=\frac{\rho^0}{V}\int_{\mathcal{A}_{\beta\gamma}}\mathbf{n}_{\beta\gamma}\cdot\tilde{\mathbf{v}}_\beta\,dA=-\frac{\rho^0}{V}\int_{\mathcal{A}_{\beta\gamma}}\mathbf{n}_{\gamma\beta}\cdot\tilde{\mathbf{v}}_\gamma\,dA. \tag{57}$$

Using the above expressions in conjunction with Eq. (30), we obtain the two coupled continuity equations

$$c\frac{\partial\langle P_\beta\rangle^\beta}{\partial t}+\nabla\cdot\langle\mathbf{v}_\beta\rangle^\beta=-\varepsilon_\beta^{-1}\frac{\dot{m}}{\rho^0}, \tag{58}$$

$$c\frac{\partial\langle P_\gamma\rangle^\gamma}{\partial t}+\nabla\cdot\langle\mathbf{v}_\gamma\rangle^\gamma=\varepsilon_\gamma^{-1}\frac{\dot{m}}{\rho^0}. \tag{59}$$

At this point of the developments, we have obtained the macroscale equations that describe mass and momentum transport within bi-structured porous media. However, these equations are not in a closed form since Eqs. (58), (59) and (54) contain terms involving the velocity and pressure fluctuations, $\tilde{p}_i$ and $\tilde{\mathbf{v}}_i$. In order to eliminate these quantities from the macroscale equations, we will follow a procedure based on closure variable decompositions (similar to Darcy's law derivation).

4.2. Deviations

The first step towards a solution is to determine the boundary value problems that describe the perturbations behavior. This may be done by subtracting Eq. (58) from Eq. (4) in order to obtain

$$\nabla\cdot\tilde{\mathbf{v}}_i=\frac{\varepsilon_i^{-1}}{V}\int_{\mathcal{A}_i}\mathbf{n}_i\cdot\tilde{\mathbf{v}}_i\,dA\quad\texttt{in } V_i\quad\texttt{where } i=\beta,\gamma. \tag{60}$$

In this equation, we have neglected terms involving $\tilde{\rho}_i$. We remark that, in the upscaling literature, most derivations make the assumption that mass exchange can be neglected at the microscale and, therefore, $\dot{m}$ may be discarded in these developments. For instance, this is the case in Whitaker (1986b, 1994) and Lasseux et al. (1996, 2008) in which the right-hand side of Eq. (60) has been eliminated. In this work, our goal is to develop a model that may be used to describe mass exchange processes so that we have kept these terms in the developments.

We can use a similar procedure for the momentum balance equation. This is done by subtracting Eq. (34) from Eq. (5) and neglecting higher order terms. The result of this operation is

$$0=-\nabla\tilde{p}_i+\mu\nabla^2\tilde{\mathbf{v}}_i-\frac{\varepsilon_i^{-1}}{V}\int_{\mathcal{A}_i}\mathbf{n}_i\cdot(-\tilde{p}_i\mathbf{I}+\mu\nabla\tilde{\mathbf{v}}_i)\,dA\quad\texttt{in } V_i\quad\texttt{with } i=\beta,\gamma, \tag{61}$$

and the no-slip boundary condition reads

$$\tilde{\mathbf{v}}_i=-\langle\mathbf{v}_i\rangle^i\quad\texttt{at } \mathcal{A}_{i\sigma},\quad i=\beta,\gamma. \tag{62}$$

Continuity conditions for pressures and velocities at the interface $\mathcal{A}_{\beta\gamma}$ supply

$$\tilde{\mathbf{v}}_\beta=\tilde{\mathbf{v}}_\gamma-(\langle\mathbf{v}_\beta\rangle^\beta-\langle\mathbf{v}_\gamma\rangle^\gamma)\quad\texttt{at } \mathcal{A}_{\beta\gamma}, \tag{63}$$

$$\tilde{p}_\beta=\tilde{p}_\gamma-(\langle p_\beta\rangle^\beta-\langle p_\gamma\rangle^\gamma)\quad\texttt{at } \mathcal{A}_{\beta\gamma}. \tag{64}$$

To ensure uniqueness of solutions, we impose the solvability condition

$$\langle\tilde{\mathbf{v}}_i\rangle^i=0\quad\text{and}\quad\langle\tilde{p}_i\rangle^i=0\quad\texttt{with } i=\beta,\gamma, \tag{65}$$

and use local periodic conditions for the deviations

$$\tilde{\mathbf{v}}_i(\mathbf{r}+\mathbf{l}_k)=\tilde{\mathbf{v}}_i(\mathbf{r})\quad\texttt{and}\quad\tilde{p}_i(\mathbf{r}+\mathbf{l}_k)=\tilde{p}_i(\mathbf{r})\quad\texttt{with } i=\beta,\gamma\quad\texttt{and}\quad k=1,2,3. \tag{66}$$

At this stage, we may identify three macroscale source terms in the above boundary value problem ($\langle\mathbf{v}_\beta\rangle^\beta$, $\langle\mathbf{v}_\gamma\rangle^\gamma$ and $\langle p_\beta\rangle^\beta-\langle p_\gamma\rangle^\gamma$). Given the linearity of the spatial operators, we can express velocity perturbations as

$$\tilde{\mathbf{v}}_\beta=\mathbf{A}_{\beta\beta}\cdot\langle\mathbf{v}_\beta\rangle^\beta+\mathbf{A}_{\beta\gamma}\cdot\langle\mathbf{v}_\gamma\rangle^\gamma+\frac{\mathbf{B}_\beta}{\mu}(\langle p_\beta\rangle^\beta-\langle p_\gamma\rangle^\gamma), \tag{67}$$

and

$$\tilde{\mathbf{v}}_\gamma=\mathbf{A}_{\gamma\beta}\cdot\langle\mathbf{v}_\beta\rangle^\beta+\mathbf{A}_{\gamma\gamma}\cdot\langle\mathbf{v}_\gamma\rangle^\gamma+\frac{\mathbf{B}_\gamma}{\mu}(\langle p_\beta\rangle^\beta-\langle p_\gamma\rangle^\gamma). \tag{68}$$

A similar decomposition for pressure perturbations can be written as

$$\tilde{p}_\beta=\mu[\mathbf{a}_{\beta\beta}\cdot\langle\mathbf{v}_\beta\rangle^\beta+\mathbf{a}_{\beta\gamma}\cdot\langle\mathbf{v}_\gamma\rangle^\gamma]+b_\beta(\langle p_\beta\rangle^\beta-\langle p_\gamma\rangle^\gamma), \tag{69}$$

$$\tilde{p}_\gamma=\mu[\mathbf{a}_{\gamma\beta}\cdot\langle\mathbf{v}_\beta\rangle^\beta+\mathbf{a}_{\gamma\gamma}\cdot\langle\mathbf{v}_\gamma\rangle^\gamma]+b_\gamma(\langle p_\beta\rangle^\beta-\langle p_\gamma\rangle^\gamma). \tag{70}$$

Similarly to Darcy's law, we will refer to $\mathbf{A}_{ij}$, $\mathbf{B}_i$, $\mathbf{a}_{ij}$ and b_i as mapping or closure variables. In these equations, $\mathbf{A}_{ij}$ are second order tensors; $\mathbf{B}_i$ and $\mathbf{a}_{ij}$ are first order tensors; and b_i are scalars. For simplicity, we have used notations similar to those adopted in Whitaker (1994) and Lasseux et al. (1996) when dealing with two-phase problems. We will see in Section 4.4.4 and Appendix B.1 that connections exist between these works and the present study; so that the corresponding boundary value problems can be expressed in a similar form and readily compared.

4.3. Equations for the closure variables

At this point, we have obtained an explicit decomposition of the perturbations that can be substituted into Eqs. (67)–(70) and into Eqs. (60)–(66) in order to decouple the mapping variables from the macroscale equations. Assuming linear independence of the source terms, we can collect terms involving $\langle\mathbf{v}_\beta\rangle^\beta$, $\langle\mathbf{v}_\gamma\rangle^\gamma$ and

$\langle p_\beta\rangle^\beta - \langle p_\gamma\rangle^\gamma$ separately. The corresponding boundary value problems are detailed below.

4.3.1. Mapping onto $\langle \mathbf{v}_\beta\rangle^\beta$ and $\langle \mathbf{v}_\gamma\rangle^\gamma$

Identification of terms involving $\langle \mathbf{v}_\beta\rangle^\beta$ yields *Problem* I

$$0 = -\nabla \mathbf{a}_{i\beta} + \nabla^2 \mathbf{A}_{i\beta} - \frac{\varepsilon_i^{-1}}{V}\int_{\mathcal{A}_i} \mathbf{n}_i\cdot(-\mathbf{I}\mathbf{a}_{i\beta} + \nabla \mathbf{A}_{i\beta})\, dA \quad \text{in } V_i \quad \text{with } i = \beta,\gamma, \tag{71}$$

and

$$\nabla\cdot\mathbf{A}_{i\beta} = \frac{\varepsilon_i^{-1}}{V}\int_{\mathcal{A}_{\gamma\beta}} \mathbf{n}_i\cdot\mathbf{A}_{i\beta}\, dA \quad \text{in } V_i \quad \text{with } i = \beta,\gamma. \tag{72}$$

The boundary conditions may be written as

$$\mathbf{A}_{\beta\beta} = -\mathbf{I} \quad \text{at } \mathcal{A}_{\beta\sigma}, \tag{73}$$

$$\mathbf{A}_{\gamma\beta} = 0 \quad \text{at } \mathcal{A}_{\gamma\sigma}, \tag{74}$$

$$\mathbf{A}_{\beta\beta} = \mathbf{A}_{\gamma\beta} - \mathbf{I} \quad \text{at } \mathcal{A}_{\beta\gamma}, \tag{75}$$

and

$$\mathbf{a}_{\beta\beta} = \mathbf{a}_{\gamma\beta} \quad \text{at } \mathcal{A}_{\beta\gamma}. \tag{76}$$

To ensure uniqueness of solutions, we also have the periodicity conditions

$$\mathbf{A}_{i\beta}(\mathbf{r} + \mathbf{l}_k) = \mathbf{A}_{i\beta}(\mathbf{r}) \quad \text{and} \quad \mathbf{a}_{i\beta}(\mathbf{r} + \mathbf{l}_k) = \mathbf{a}_{i\beta}(\mathbf{r}) \quad \text{with } i = \beta,\gamma \quad \text{and} \quad k = 1,2,3, \tag{77}$$

and the solvability conditions

$$\langle \mathbf{A}_{i\beta}\rangle^i = 0 \quad \text{and} \quad \langle \mathbf{a}_{i\beta}\rangle^i = 0 \quad \text{with } i = \beta,\gamma. \tag{78}$$

Similarly, identification of terms involving $\langle \mathbf{v}_\gamma\rangle^\gamma$ yields *Problem* II

$$0 = -\nabla \mathbf{a}_{i\gamma} + \nabla^2 \mathbf{A}_{i\gamma} - \frac{\varepsilon_i^{-1}}{V}\int_{\mathcal{A}_i} \mathbf{n}_i\cdot(-\mathbf{I}\mathbf{a}_{i\gamma} + \nabla \mathbf{A}_{i\gamma})\, dA \quad \text{in } V_i \quad \text{with } i = \beta,\gamma, \tag{79}$$

and

$$\nabla.\mathbf{A}_{i\gamma} = \frac{\varepsilon_i^{-1}}{V}\int_{\mathcal{A}_{\gamma\beta}} \mathbf{n}_i\cdot\mathbf{A}_{i\gamma}\, dA \quad \text{in } V_i \quad \text{with } i = \beta,\gamma. \tag{80}$$

The boundary conditions may be written as

$$\mathbf{A}_{\beta\gamma} = 0 \quad \text{at } \mathcal{A}_{\beta\sigma}, \tag{81}$$

$$\mathbf{A}_{\gamma\gamma} = -\mathbf{I} \quad \text{at } \mathcal{A}_{\gamma\sigma}, \tag{82}$$

$$\mathbf{A}_{\beta\gamma} = \mathbf{A}_{\gamma\gamma} + \mathbf{I} \quad \text{at } \mathcal{A}_{\beta\gamma}, \tag{83}$$

and

$$\mathbf{a}_{\beta\gamma} = \mathbf{a}_{\gamma\gamma} \quad \text{at } \mathcal{A}_{\beta\gamma}. \tag{84}$$

To ensure uniqueness of solutions, we also have the periodicity conditions

$$\mathbf{A}_{i\gamma}(\mathbf{r} + \mathbf{l}_k) = \mathbf{A}_{i\gamma}(\mathbf{r}) \quad \text{and} \quad \mathbf{a}_{i\gamma}(\mathbf{r} + \mathbf{l}_k) = \mathbf{a}_{i\gamma}(\mathbf{r}) \quad \text{with } i = \beta,\gamma \quad \text{and} \quad k = 1,2,3, \tag{85}$$

and the solvability conditions

$$\langle \mathbf{A}_{i\gamma}\rangle^i = 0; \quad \langle \mathbf{a}_{i\gamma}\rangle^i = 0 \quad \text{with } i = \beta,\gamma. \tag{86}$$

Apart from the additional exchange terms in the continuity equations, these closure problems are similar to those derived by Whitaker (1994) in the case of two-phase flow in homogeneous porous media. Following this paper, we define permeabilities $\mathbf{K}_\beta$ and $\mathbf{K}_\gamma$ and coupling tensors $\mathbf{K}_{\gamma\beta}$ and $\mathbf{K}_{\beta\gamma}$ as

$$\varepsilon_\beta \mathbf{K}_\beta^{-1} = -\frac{\varepsilon_\beta^{-1}}{V}\int_{\mathcal{A}_\beta} \mathbf{n}_\beta\cdot(-\mathbf{I}\mathbf{a}_{\beta\beta} + \nabla \mathbf{A}_{\beta\beta})\, dA, \tag{87}$$

$$\varepsilon_\gamma \mathbf{K}_\beta^{-1}\cdot\mathbf{K}_{\beta\gamma} = \frac{\varepsilon_\beta^{-1}}{V}\int_{\mathcal{A}_\beta} \mathbf{n}_\beta\cdot(-\mathbf{I}\mathbf{a}_{\beta\gamma} + \nabla \mathbf{A}_{\beta\gamma})\, dA, \tag{88}$$

$$\varepsilon_\beta \mathbf{K}_\gamma^{-1}\cdot\mathbf{K}_{\gamma\beta} = \frac{\varepsilon_\gamma^{-1}}{V}\int_{\mathcal{A}_\gamma} \mathbf{n}_\gamma\cdot(-\mathbf{I}\mathbf{a}_{\gamma\beta} + \nabla \mathbf{A}_{\gamma\beta})\, dA, \tag{89}$$

and

$$\varepsilon_\gamma \mathbf{K}_\gamma^{-1} = -\frac{\varepsilon_\gamma^{-1}}{V}\int_{\mathcal{A}_\gamma} \mathbf{n}_\gamma\cdot(-\mathbf{I}\mathbf{a}_{\gamma\gamma} + \nabla \mathbf{A}_{\gamma\gamma})\, dA. \tag{90}$$

These definitions, although not necessarily obvious at first, significantly facilitate future mathematical developments of the macroscale equations. Further, following Lasseux et al. (1996), we will use $\mathbf{K}^*_{\beta\beta}$, $\mathbf{K}^*_{\beta\gamma}$, $\mathbf{K}^*_{\gamma\gamma}$ and $\mathbf{K}^*_{\gamma\beta}$ which are defined by

$$\mathbf{K}^*_{\beta\beta} = (\mathbf{I} - \mathbf{K}_{\beta\gamma}\cdot\mathbf{K}_{\gamma\beta})^{-1}\cdot\mathbf{K}_\beta, \tag{91}$$

$$\mathbf{K}^*_{\beta\gamma} = (\mathbf{I} - \mathbf{K}_{\beta\gamma}\cdot\mathbf{K}_{\gamma\beta})^{-1}\cdot\mathbf{K}_{\beta\gamma}\cdot\mathbf{K}_\gamma, \tag{92}$$

$$\mathbf{K}^*_{\gamma\gamma} = (\mathbf{I} - \mathbf{K}_{\gamma\beta}\cdot\mathbf{K}_{\beta\gamma})^{-1}\cdot\mathbf{K}_\gamma, \tag{93}$$

and

$$\mathbf{K}^*_{\gamma\beta} = (\mathbf{I} - \mathbf{K}_{\gamma\beta}\cdot\mathbf{K}_{\beta\gamma})^{-1}\cdot\mathbf{K}_{\gamma\beta}\cdot\mathbf{K}_\beta. \tag{94}$$

We will also use

$$\chi_{ij} = \frac{1}{V}\int_{\mathcal{A}_{\gamma\beta}} \mathbf{n}_i\cdot\mathbf{A}_{ij}\, dA \quad \text{with } i,j = \beta,\gamma, \tag{95}$$

and the relations

$$\chi_{\beta\beta} = -\chi_{\gamma\beta} \quad \text{and} \quad \chi_{\beta\gamma} = -\chi_{\gamma\gamma}. \tag{96}$$

4.3.2. Mapping onto $\langle p_\beta\rangle^\beta - \langle p_\gamma\rangle^\gamma$

Collecting terms involving $\langle p_\beta\rangle^\beta - \langle p_\gamma\rangle^\gamma$ yields *Problem* III

$$0 = -\nabla b_i + \nabla^2 \mathbf{B}_i - \mathbf{K}_i^{-1}\cdot\mathbf{\Pi}_i \quad \text{in } V_i \quad \text{with } i = \beta,\gamma, \tag{97}$$

$$\nabla\cdot\mathbf{B}_\beta = \varepsilon_\beta^{-1} h \quad \text{in } V_\beta, \tag{98}$$

$$\nabla\cdot\mathbf{B}_\gamma = -\varepsilon_\gamma^{-1} h \quad \text{in } V_\gamma, \tag{99}$$

with the boundary conditions

$$\mathbf{B}_i = 0 \quad \text{at } \mathcal{A}_{i\sigma} \quad \text{with } i = \beta,\gamma, \tag{100}$$

$$\mathbf{B}_\beta = \mathbf{B}_\gamma \quad \text{at } \mathcal{A}_{\beta\gamma}, \tag{101}$$

$$b_\beta = b_\gamma - 1 \quad \text{at } \mathcal{A}_{\beta\gamma}. \tag{102}$$

Uniqueness of solutions is also ensured by local periodicity, i.e.,

$$\mathbf{B}_i(\mathbf{r} + \mathbf{l}_k) = \mathbf{B}_i(\mathbf{r}) \quad \text{and} \quad b_i(\mathbf{r} + \mathbf{l}_k) = b_i(\mathbf{r}) \quad \text{with } i = \beta,\gamma \quad \text{and} \quad k = 1,2,3, \tag{103}$$

and the solvability conditions

$$\langle \mathbf{B}_i\rangle^i = 0; \quad \langle b_i\rangle^i = 0 \quad \text{with } i = \beta,\gamma. \tag{104}$$

In these equations, we have used the notations

$$\mathbf{K}_i^{-1}\cdot\mathbf{\Pi}_i = -\frac{\varepsilon_i^{-1}}{V}\int_{\mathcal{A}_i} \mathbf{n}_i\cdot(-b_i\mathbf{I} + \nabla \mathbf{B}_i)\, dA, \tag{105}$$

and

$$h = \frac{1}{V}\int_{\mathcal{A}_{\beta\gamma}} \mathbf{n}_{\beta\gamma}\cdot\mathbf{B}_\beta\, dA = -\frac{1}{V}\int_{\mathcal{A}_{\beta\gamma}} \mathbf{n}_{\gamma\beta}\cdot\mathbf{B}_\gamma\, dA. \tag{106}$$

We have also defined $\boldsymbol{\Pi}_i^*$ as

$$\boldsymbol{\Pi}_\beta^* = (\mathbf{I} - \mathbf{K}_{\beta\gamma}\cdot\mathbf{K}_{\gamma\beta})^{-1}\cdot(\Pi_\beta + \mathbf{K}_{\beta\gamma}\cdot\boldsymbol{\Pi}_\gamma), \tag{107}$$

and

$$\Pi_\gamma^* = (\mathbf{I} - \mathbf{K}_{\gamma\beta}\cdot\mathbf{K}_{\beta\gamma})^{-1}\cdot(\boldsymbol{\Pi}_\gamma + \mathbf{K}_{\gamma\beta}\cdot\Pi_\beta). \tag{108}$$

4.4. Macroscale models

Herein, we use the above developments and the expressions of the deviations to obtain closed forms of the macroscale equations.

4.4.1. Macroscale equations for regional velocities

To obtain macroscale equations for regional velocities, we use Eqs. (67)–(70) into Eq. (54) and multiply each equation by $\mathbf{K}_i$. The result of this operation is

$$\langle \mathbf{v}_\beta\rangle = -\frac{\mathbf{K}_\beta}{\mu}\cdot(\nabla\langle p_\beta\rangle^\beta - \langle\rho_\beta\rangle^\beta\mathbf{g}) + \mathbf{K}_{\beta\gamma}\cdot\langle\mathbf{v}_\gamma\rangle + \boldsymbol{\Pi}_\beta(\langle p_\beta\rangle^\beta - \langle p_\gamma\rangle^\gamma), \tag{109}$$

and

$$\langle \mathbf{v}_\gamma\rangle = -\frac{\mathbf{K}_\gamma}{\mu}\cdot(\nabla\langle p_\gamma\rangle^\gamma - \langle\rho_\gamma\rangle^\gamma\mathbf{g}) + \mathbf{K}_{\gamma\beta}\cdot\langle\mathbf{v}_\beta\rangle + \boldsymbol{\Pi}_\gamma(\langle p_\beta\rangle^\beta - \langle p_\gamma\rangle^\gamma). \tag{110}$$

Further, we can use hydrostatic pressures and simple linear algebra to obtain

$$\langle \mathbf{v}_\beta\rangle = -\frac{\mathbf{K}_{\beta\beta}^*}{\mu}\cdot\nabla\langle P_\beta\rangle^\beta - \frac{\mathbf{K}_{\beta\gamma}^*}{\mu}\cdot\nabla\langle P_\gamma\rangle^\gamma + \boldsymbol{\Pi}_\beta^*(\langle P_\beta\rangle^\beta - \langle P_\gamma\rangle^\gamma), \tag{111}$$

and

$$\langle \mathbf{v}_\gamma\rangle = -\frac{\mathbf{K}_{\gamma\beta}^*}{\mu}\cdot\nabla\langle P_\beta\rangle^\beta - \frac{\mathbf{K}_{\gamma\gamma}^*}{\mu}\cdot\nabla\langle P_\gamma\rangle^\gamma + \boldsymbol{\Pi}_\gamma^*(\langle P_\beta\rangle^\beta - \langle P_\gamma\rangle^\gamma). \tag{112}$$

We remark that these equations are similar to those derived in Quintard and Whitaker (1998) for the large scale averaging of Darcy's law in heterogeneous porous media. However, (1) the macroscale equations obtained in Quintard and Whitaker (1998) apply to the large-scale whereas our developments apply to the Darcy-scale and (2) the derivation in Quintard and Whitaker (1998) is based on the upscaling of Darcy's law whereas our developments are based on the upscaling of Stokes problem. Therefore, effective parameters have a different micro-scale definition.

4.4.2. Macroscale continuity equations and mass exchange rate

Recall that the mass balance equations derived in Section 4 read

$$\varepsilon_\beta c\frac{\partial\langle P_\beta\rangle^\beta}{\partial t} + \nabla\cdot\langle\mathbf{v}_\beta\rangle = -\frac{\dot m}{\rho^0}, \tag{113}$$

and

$$\varepsilon_\gamma c\frac{\partial\langle P_\gamma\rangle^\gamma}{\partial t} + \nabla\cdot\langle\mathbf{v}_\gamma\rangle = \frac{\dot m}{\rho^0}. \tag{114}$$

A closed form of the mass exchange rate, $\dot m$, can be obtained by substituting Eq. (67) into Eq. (57)

$$\frac{\dot m}{\rho^0} = -\boldsymbol{\chi}_{\gamma\beta}\cdot\langle\mathbf{v}_\beta\rangle + \boldsymbol{\chi}_{\beta\gamma}\cdot\langle\mathbf{v}_\gamma\rangle + \frac{h}{\mu}(\langle P_\beta\rangle^\beta - \langle P_\gamma\rangle^\gamma). \tag{115}$$

We can further use the expressions of the regional velocities, Eqs. (111) and (112), to obtain

$$\frac{\dot m}{\rho^0} = -\boldsymbol{\chi}_{\gamma\beta}^*\cdot\nabla\langle P_\beta\rangle^\beta + \boldsymbol{\chi}_{\beta\gamma}^*\cdot\nabla\langle P_\gamma\rangle^\gamma + \frac{h^*}{\mu}\left(\langle P_\beta\rangle^\beta - \langle P_\gamma\rangle^\gamma\right), \tag{116}$$

where

$$h^* = h - \mu\varepsilon_\beta^{-1}\boldsymbol{\chi}_{\gamma\beta}\cdot\boldsymbol{\Pi}_\beta^* + \mu\varepsilon_\gamma^{-1}\boldsymbol{\chi}_{\beta\gamma}\cdot\boldsymbol{\Pi}_\gamma^*, \tag{117}$$

$$\boldsymbol{\chi}_{\gamma\beta}^* = -\varepsilon_\beta^{-1}\boldsymbol{\chi}_{\gamma\beta}\cdot\frac{\mathbf{K}_{\beta\beta}^*}{\mu} + \varepsilon_\gamma^{-1}\boldsymbol{\chi}_{\beta\gamma}\cdot\frac{\mathbf{K}_{\gamma\beta}^*}{\mu}, \tag{118}$$

and

$$\boldsymbol{\chi}_{\beta\gamma}^* = -\varepsilon_\beta^{-1}\boldsymbol{\chi}_{\gamma\beta}\cdot\frac{\mathbf{K}_{\beta\gamma}^*}{\mu} + \varepsilon_\gamma^{-1}\boldsymbol{\chi}_{\beta\gamma}\cdot\frac{\mathbf{K}_{\gamma\gamma}^*}{\mu}. \tag{119}$$

4.4.3. Macroscale equations for the pressure

We form the macroscale equations that govern the pressure fields by using Eqs. (111), (112) and (116) into Eqs. (58) and (59). This leads to the following two-pressure model with mass exchange

$$\begin{aligned}\varepsilon_\beta c\frac{\partial\langle P_\beta\rangle^\beta}{\partial t} - \boldsymbol{\chi}_{\gamma\beta}^*\cdot\nabla\langle P_\beta\rangle^\beta + \boldsymbol{\chi}_{\beta\gamma}^*\cdot\nabla\langle P_\gamma\rangle^\gamma + \nabla\cdot(\boldsymbol{\Pi}_\beta^*(\langle P_\beta\rangle^\beta - \langle P_\gamma\rangle^\gamma))\\ = \nabla\cdot\left(\frac{\mathbf{K}_{\beta\beta}^*}{\mu}\cdot\nabla\langle P_\beta\rangle^\beta\right) + \nabla\cdot\left(\frac{\mathbf{K}_{\beta\gamma}^*}{\mu}\cdot\nabla\langle P_\gamma\rangle^\gamma\right) - \frac{h^*}{\mu}(\langle P_\beta\rangle^\beta - \langle P_\gamma\rangle^\gamma),\end{aligned} \tag{120}$$

$$\begin{aligned}\varepsilon_\gamma c\frac{\partial\langle P_\gamma\rangle^\gamma}{\partial t} + \boldsymbol{\chi}_{\gamma\beta}^*\cdot\nabla\langle P_\beta\rangle^\beta - \boldsymbol{\chi}_{\beta\gamma}^*\cdot\nabla\langle P_\gamma\rangle^\gamma + \nabla\cdot(\boldsymbol{\Pi}_\gamma^*(\langle P_\beta\rangle^\beta - \langle P_\gamma\rangle^\gamma))\\ = \nabla\cdot\left(\frac{\mathbf{K}_{\gamma\beta}^*}{\mu}\cdot\nabla\langle P_\beta\rangle^\beta\right) + \nabla\cdot\left(\frac{\mathbf{K}_{\gamma\gamma}^*}{\mu}\cdot\nabla\langle P_\gamma\rangle^\gamma\right) + \frac{h^*}{\mu}(\langle P_\beta\rangle^\beta - \langle P_\gamma\rangle^\gamma).\end{aligned} \tag{121}$$

Effective properties of this model can be determined by resolution of the three integro-differential problems derived in Section 4. Because of the complexity involved, we develop in the next section a method to evaluate the effective properties for the simpler case in which the mass exchange term depends only on the average pressure difference.

4.4.4. Simplified macroscale model

In this section, we propose further simplifications of the above macroscale equations. At leading order, $\dot m$ is governed by the pressure difference and can be approximated, following Eq. (116), by:

$$\frac{\dot m}{\rho^0} \approx \frac{h}{\mu}(\langle P_\beta\rangle^\beta - \langle P_\gamma\rangle^\gamma). \tag{122}$$

In this case, χ_{ij} in Eqs. (120) and (121) are neglected and the continuity equations in the closure Problems I and II become divergence-free. Furthermore, we remark that several closure problems developed in this work (see Appendix B.1) may simplify to those derived for the two-phase flow configuration (see Whitaker, 1986a, 1994 or Lasseux et al., 1996), so that the macroscale parameters $\mathbf{K}_{ij}^*$ can be determined directly from the mapping fields of the two-phase flow problem. In addition, the values of the exchange parameters h and $\boldsymbol{\Pi}_i^*$ may be directly

Table 1
Comparison of the upscaling procedure used in Quintard and Whitaker (1996) with the present work. In the former study, the authors investigated fluid flow through heterogeneous porous media described at a "large-scale". They first averaged Stokes problem to form Darcy's law and then averaged Darcy's law on a larger scale to obtain the two-pressure model. In the present study, we directly derive a two-pressure model at the Darcy-scale from Stokes equations. Therefore, our model is an alternative to the classical Darcy's law and covers a larger set of bi-structured media including systems for which the two-step upscaling procedure is not possible.

Scale	Quintard and Whitaker (1996)	Present work
Pore-scale	Stokes problem	Stokes problem
Darcy-scale	One-pressure model (Darcy's law)	Two-pressure model
	closure: pore-scale, one problem	closure: pore-scale, 3 problems
Large-scale	Two-pressure model	–
	closure: Darcy-scale, 3 problems	

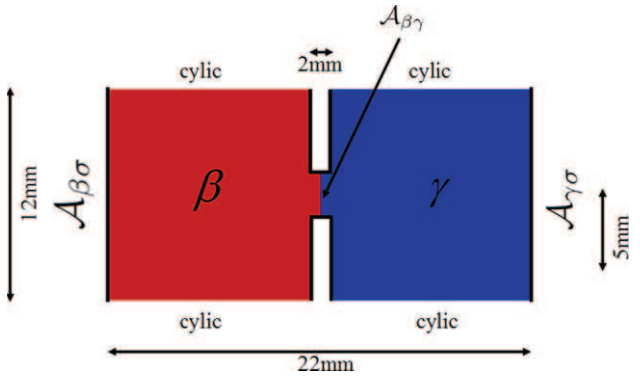

Fig. 4. Schematics of the unit-cell geometry, the two-regions and the boundaries.

determined using a transformation of the integro-differential Problem III (see Appendix B.2). With this approximation (Eq. (122)) the macroscale model for the averaged pressures becomes

$$\varepsilon_\beta c\frac{\partial\langle P_\beta\rangle^\beta}{\partial t}+\nabla\cdot(\mathbf{\Pi}_\beta^*(\langle P_\beta\rangle^\beta-\langle P_\gamma\rangle^\gamma))=\nabla\cdot\left(\frac{\mathbf{K}_{\beta\beta}^*}{\mu}\cdot\nabla\langle P_\beta\rangle^\beta\right)+\nabla\cdot\left(\frac{\mathbf{K}_{\beta\gamma}^*}{\mu}\cdot\nabla\langle P_\gamma\rangle^\gamma\right)-\frac{h}{\mu}(\langle P_\beta\rangle^\beta-\langle P_\gamma\rangle^\gamma),\tag{123}$$

$$\varepsilon_\gamma c\frac{\partial\langle P_\gamma\rangle^\gamma}{\partial t}+\nabla\cdot(\mathbf{\Pi}_\gamma^*(\langle P_\beta\rangle^\beta-\langle P_\gamma\rangle^\gamma))=\nabla\cdot\left(\frac{\mathbf{K}_{\gamma\beta}^*}{\mu}\cdot\nabla\langle P_\beta\rangle^\beta\right)+\nabla\cdot\left(\frac{\mathbf{K}_{\gamma\gamma}^*}{\mu}\cdot\nabla\langle P_\gamma\rangle^\gamma\right)+\frac{h}{\mu}(\langle P_\beta\rangle^\beta-\langle P_\gamma\rangle^\gamma).\tag{124}$$

This model is reminiscent of the developments of Quintard and Whitaker (1996) for the problem of flow through heterogeneous porous media with a two-step upscaling procedure (Stokes to Darcy and Darcy to large-scale). An interesting feature of the present work is to provide a solid theoretical framework for the *direct* derivation of this model with a one-step averaging procedure from the pore-scale Stokes problem. As a consequence, effective properties in the proposed model are obtained from a completely different closure involving pore-scale instead of Darcy-scale characteristics. Table 1 summarizes the comparison between the two developments.

Furthermore, if we consider a case for which the coupling terms are relatively small, i.e., if $\mathbf{K}_{\gamma\beta}^*,\mathbf{K}_{\beta\gamma}^*\ll\mathbf{K}_{\gamma\gamma}^*,\mathbf{K}_{\beta\beta}^*$, and the $\mathbf{\Pi}_i^*$ can be neglected, we recover exactly the model proposed empirically by Barenblatt et al. (1960) for larger scales

$$c\varepsilon_\beta\frac{\partial\langle P_\beta\rangle^\beta}{\partial t}=\nabla\cdot\left(\frac{\mathbf{K}_\beta}{\mu}\cdot\nabla\langle P_\beta\rangle^\beta\right)-\frac{h}{\mu}(\langle P_\beta\rangle^\beta-\langle P_\gamma\rangle^\gamma),\tag{125}$$

$$c\varepsilon_\gamma\frac{\partial\langle P_\gamma\rangle^\gamma}{\partial t}=\nabla\cdot\left(\frac{\mathbf{K}_\gamma}{\mu}\cdot\nabla\langle P_\gamma\rangle^\gamma\right)+\frac{h}{\mu}(\langle P_\beta\rangle^\beta-\langle P_\gamma\rangle^\gamma).\tag{126}$$

5. Validation against direct numerical simulations for a simplified particle filter

In order to illustrate the proposed theory, we apply it in this section to a 2D model problem which may be thought of as a simplified particle tangential filter. Our goal is to examine numerically the applicability of the two-pressure model to the flow of an incompressible and a slightly compressible fluid within this particle filter. We will present solutions of the two- and one-pressure models and compare these macroscale results with the solution of the microscale problem. Computations were all performed with the finite volume CFD toolbox OpenFOAM®.

5.1. Microscale geometry and models

The 2D geometry of the porous structure consists of a succession of 32 identical elements or unit-cells (see Fig. 4). The mesh contains 358 400 hexahedral cells, i.e., 11 200 cells per representative elementary volume. For boundary conditions, we impose a Dirichlet condition for the velocity $\mathbf{v}_0$ or pressure p_{inlet} at the top left, a Dirichlet condition for pressure p_0 at the bottom right and no-slip conditions everywhere else. Note that, if the velocity and pressure conditions were applied to the entire top and bottom boundaries, we would generate a classical quasi-steady flow which could be described by a *single macroscale Darcy-equation*. In our case, the velocity and pressure boundary conditions induce an exchange flux between both left and right domains. Therefore, we split the porous medium into two distinct regions: the left hand-side $\beta-$region with the input velocity condition and the right hand-side $\gamma-$region with the output pressure boundary condition.

Incompressible fluid. We will first focus on the case of an incompressible fluid flow at steady-state. The purpose of these simulations is to illustrate that the two-pressure formulation may be necessary even at steady-state, in order to capture non-equilibrium effects induced by the boundary conditions. In conjunction with Stokes equation (with negligible gravitational effects) and the boundary conditions described above, we use the following continuity equation for an incompressible fluid:

$$\nabla\cdot\mathbf{v}_\alpha=0\quad\text{in } V_\alpha,\tag{127}$$

where $\mathbf{v}_\alpha$ is the velocity field in the whole domain. We use the following set of parameters $\mathbf{v}_0=10^{-5}$ m/s, $\rho=10^3$ kg/m^3, $\mu=10^{-3}$ kg/m/s. For these parameters, we calculated a Reynolds number of $\approx$0.1 which is in the creeping flow regime and is therefore in agreement with the assumptions of our model. Since the flow is assumed to be at steady-state, we used the SIMPLE pressure–velocity coupling procedure developed by Patankar (1980) to solve the Stokes problem.

Slightly compressible fluid. As a second step, we test our theory in the case of a slightly compressible fluid flowing through the "particle filter". The pore-scale simulations are obtained by solving the transient boundary value problem described in Section 2.1 by Eqs. (1)–(3). The pore-scale thermodynamical law reads

$$\rho_\alpha=\rho^0[1+c(p_\alpha-p^0)],\tag{128}$$

where the reference pressure, the compressibility coefficient and the reference density are $p^0=0$ kg/m/s^2, $c=0.55$ and $\rho^0=10^3$ kg/m^3, respectively. As for the incompressible case, the fluid viscosity is $\mu=10^{-3}$ kg/m/s. The problem is solved using a PISO algorithm (Issa, 1985). To avoid complications regarding acoustic waves propagation in porous media, which is beyond the scope of this paper (readers interested in such phenomena can refer to Bourbié et al., 1987), we consider a pressure ramp at the input of the device, $p_{inlet}=p_{inlet}^0(1-e^{-t/\tau})$ with $p_{inlet}^0=10^{-4}$ kg/m/s^2, $\tau=100$ s and zero initial conditions. We run calculations up to 600 s which correspond to fully established steady state regimes.

5.2. Effective properties, macroscale geometry and models

The macroscale geometry that corresponds to the 2D filter is a 1D segment, 0.384 m long, containing 32 cells. The first step towards solution is to evaluate the effective properties from the resolution of the closure Problems I′, II′ and III′ provided in Appendix B over the unit-cell (Fig. 4). OpenFOAM® and a SIMPLE algorithm were used to obtain: $\Pi_{\beta_y}^*=-\Pi_{\gamma_y}^*=4\times10^{-16}$ m^2 s/kg, $h=7.8\times10^{-4}$, $\mathrm{K}_{\beta\beta_{yy}}^*=\mathrm{K}_{\gamma\gamma_{yy}}^*=4.1\times10^{-6}$ m^2 and $\mathrm{K}_{\beta\gamma_{yy}}^*=\mathrm{K}_{\gamma\beta_{yy}}^*=1.3\times10^{-9}$ m^2 (where y is the streamwise direction). We remark that the terms $\mathrm{K}_{\beta\gamma_{yy}}^*$, $\mathrm{K}_{\gamma\beta_{yy}}^*$ and $\mathbf{\Pi}_\alpha^*$ are relatively small and play a minor role in this particular case (something we have verified

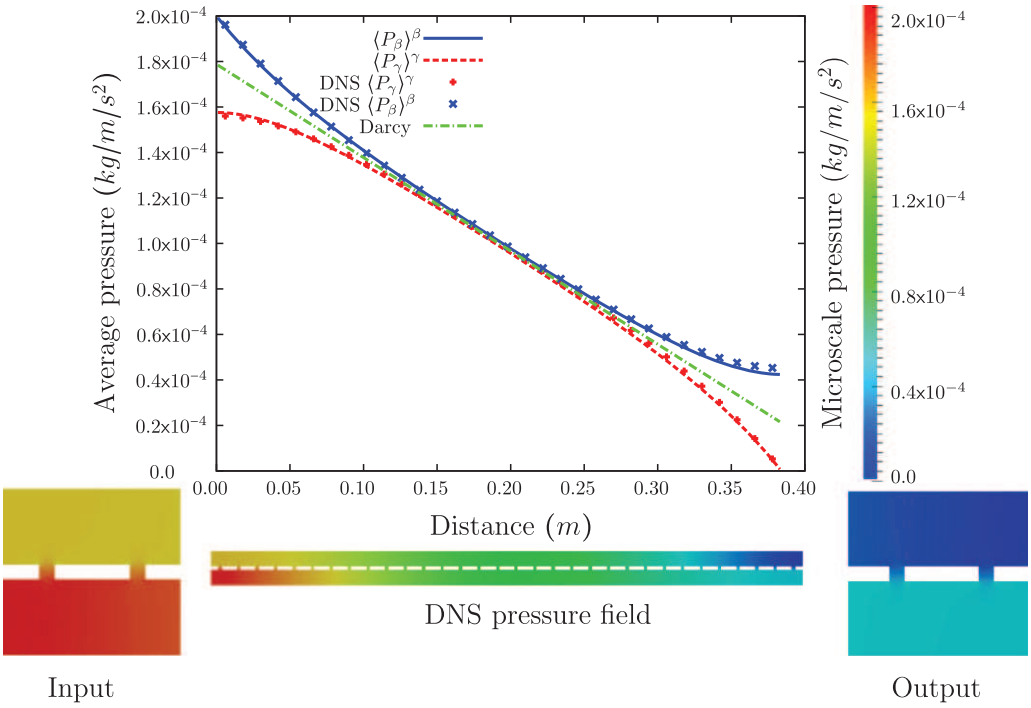

Fig. 5. Plots of the average pressure fields (top) and of the microscale pressure field (bottom) along the filter. This figure shows that: (1) both macroscale and average DNS results are in good agreement and (2) Darcy's model fails to describe non-equilibrium effects induced by boundary conditions.

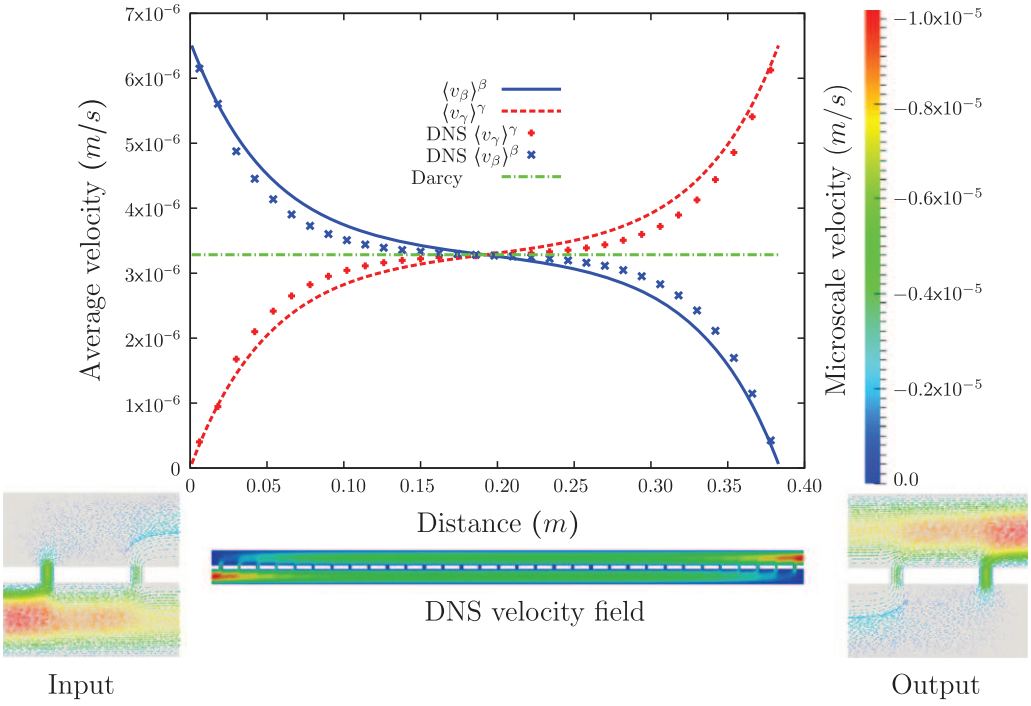

Fig. 6. Plots of the average velocity fields (top) and of the microscale velocity field (bottom) along the filter. This figure shows that: (1) both macroscale and average DNS results are in good agreement and (2) Darcy's model fails to describe non-equilibrium effects induced by boundary conditions.

numerically), something which is not general as will be emphasized in Section 6 for a different unit-cell geometry. In the incompressible case, the one-dimensional steady-state set of coupled equations (123) and (124) is solved while in the slightly compressible case we use its one-dimensional transient formulation. In both cases, these equations are solved sequentially and the regional velocities are obtained via Eqs. (109) and (110). Boundary conditions are analogous to the microscopic ones. Their values are adjusted to correspond to the average values in the vicinity of the inlet and outlet of the microscale models (Prat, 1989).

5.3. *Results for the incompressible flow*

Results for the pressure and velocity fields are plotted in Figs. 5 and 6, respectively. The average direct numerical simulation (DNS) curves were obtained by explicitly solving the microscale

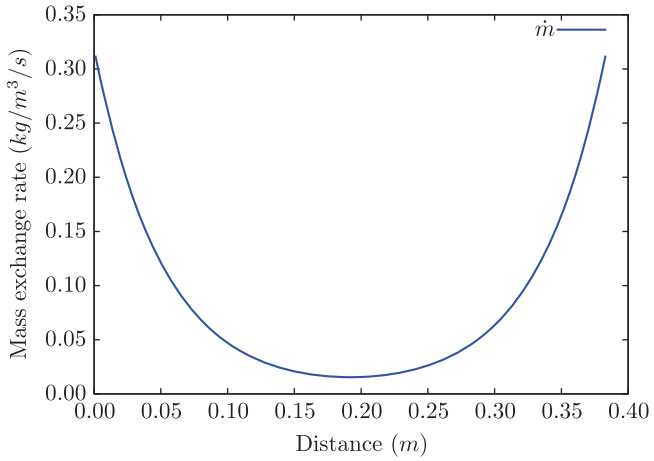

Fig. 7. Plot of the mass exchange term ($\dot{m}$) along the vertical axis. This figure shows that a local non-equilibrium situation is generated by the inlet and outlet boundaries.

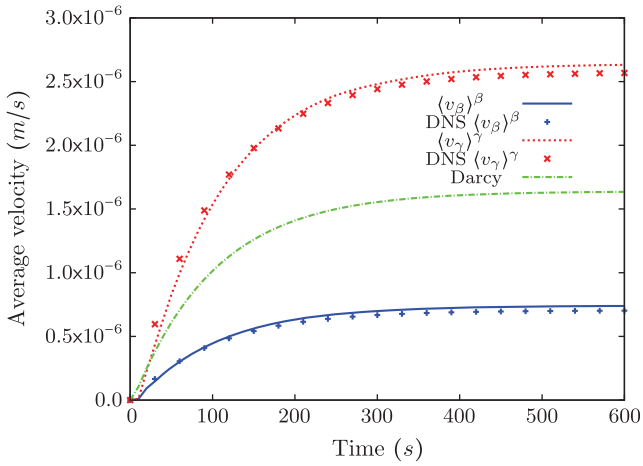

Fig. 9. Plots of the evolution of the average velocity magnitude for the 30th cell. This figure shows that the two-pressure model captures correctly the transient behavior of the average velocity.

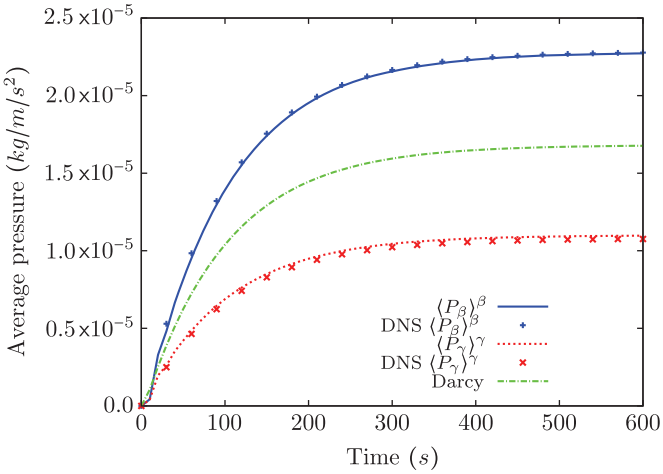

Fig. 8. Plots of the evolution of the average pressure for the 30th cell. This figure shows that the two-pressure model captures correctly the transient behavior of the average pressure.

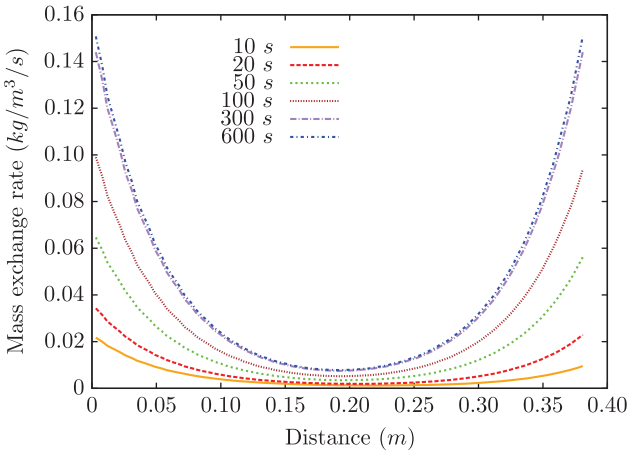

Fig. 10. Plot of the mass exchange coefficient, $\dot{m}$, along the vertical axis for several simulation times. This figure shows that non-equilibrium rapidly grows in the vicinity of the inlet and outlet boundaries.

problem presented in Section 5.1 and then volume averaging the pressure/velocity fields within the β and γ regions over each unit-cell. These results will be considered as an exact solution of the problem and serve as a reference for comparison. Macroscale pressures were obtained by solving Eqs. (123) and (124) at steady-state and velocities were determined using Eqs. (109) and (110).

As mass, momentum and pressure are exchanged between the two domains, we see in Fig. 6 that the magnitude of the velocity field in the $\beta-$region decreases along the y-axis while it increases in the $\gamma-$region. In the middle, because of the symmetry of the problem, the velocity fields of both regions are equal. This situation is usually referred to as local equilibrium in the multi-scale analysis literature. Similarly, the pressure also equilibrates in the middle (see Fig. 5). In both cases, we remark that the two-pressure model provides an excellent representation of the particle filter as average pressure and velocity fields are in very good agreement. This simulation also emphasizes the importance of the boundary conditions and illustrates the fact that non-equilibrium of velocity/pressure fields may result from a choice of particular boundary conditions, even at steady-state. This non-equilibrium effect is particularly obvious in Fig. 7 in which we have plotted the mass exchange rate, $\dot{m}$, defined by Eq. (122), as a function of y. The largest values of the mass exchange rate are at the top and the bottom of the system, where boundary conditions are important, and we have $\dot{m} \approx 0$ in the middle where both average pressure/velocity fields are almost equal.

In addition, we also remark that such non-equilibrium effects cannot be captured by a one-pressure model and the corresponding single Darcy's law. Indeed, the Darcy velocity is constant along the particle filter because the velocity field is divergence free in the macroscale continuity equation. Hence, this model will fail to describe exchange phenomena between the two regions and is not adapted to the description of flow within this specific structure. This may further impact the evaluation of heat and solute dispersion within such systems; information that are particularly useful to engineers in the field.

5.4. *Results for the slightly compressible flow*

We finally analyze the case of a slightly compressible fluid and use a similar methodology to compare results of macroscale and microscale simulations. Since our goal here is to assess the behavior of the two-pressure model in a transient situation, we will primarily focus on time representations of average values evaluated at a fixed point of space for the two-pressure, one-pressure and DNS models. Average pressure and velocity values are plotted in Figs. 8 and 9 for the 30th cell. Results show that the overall agreement between the two-

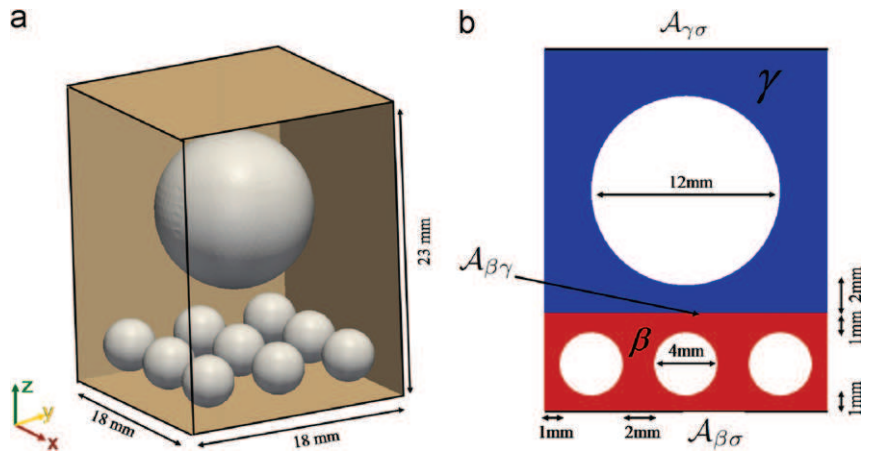

Fig. 11. (a) Schematics of the 3D unit-cell geometry and its dimensions and (b) description of the phase splitting.

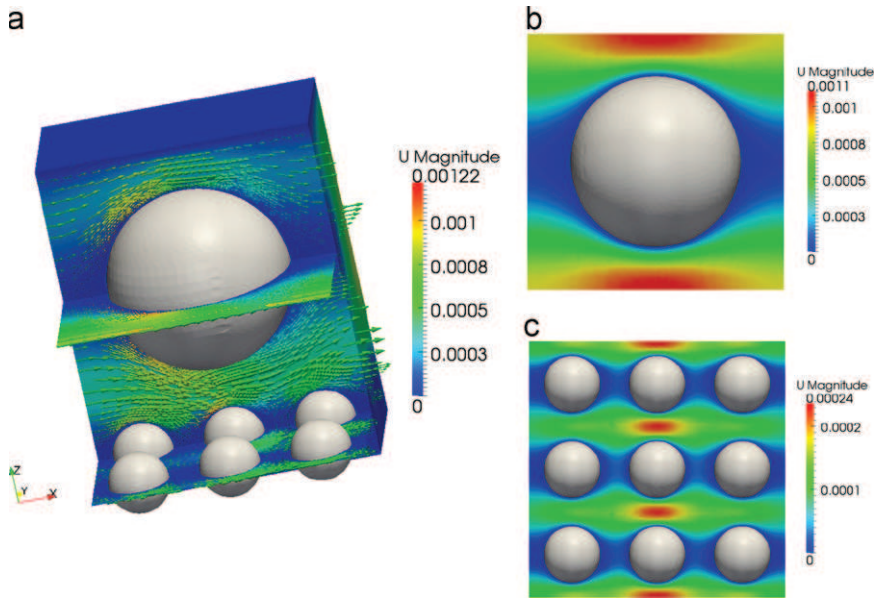

Fig. 12. The velocity field within the unit-cell (a) exhibits a large distribution in which amplitudes vary from 0 to 1.2×10^{-3} m/s. Further, the distribution is bi-modal as amplitudes in the top layer (b) are about 10 times larger than in the vicinity of the smaller beads (c).

pressure model and the DNS results is excellent. In Fig. 10, we have plotted the mass exchange rate along the vertical axis for several times, to illustrate the evolution of the non-equilibrium conditions. Because of the zero initial conditions used here, we remark that local non-equilibrium rapidly appears in the vicinity of the input and the output boundary conditions.

6. Potential importance of coupling cross-terms

In the previous section, we have shown that the two-pressure macroscale model can capture non-equilibrium phenomena induced by boundary conditions. In this application, the area of the interface which separates both pseudo-phases was small compared with the size of the unit-cell and the flow through the $\beta\gamma-$interface was mainly perpendicular to the interface. As a consequence, the coupling terms $\mathbf{K}^*_{\gamma\beta}$ and $\mathbf{K}^*_{\beta\gamma}$ were negligible. However, this might not be the case in all configurations and, to emphasize the importance of these coupling terms, we have performed simulations for a dual porous medium model as suggested in Fig. 2. This geometry does not reproduce an actual system and was essentially chosen to enhance viscous interaction between the split phases.

6.1. Geometry and phase splitting

The geometry of the 3D unit-cell used in this section (see in Fig. 11a) consists of solid impermeable beads embedded within a rectangular cuboid (18 mm × 18 mm × 23 mm). Two layers of beads are superimposed. The bottom layer contains nine small beads of equal size (radius = 2 mm) that are regularly arranged in the same *xOy* section. The top layer contains a single larger bead (radius = 6 mm). The total porosity (fluid volume fraction) of this system was estimated as $\varepsilon \approx 0.84$. Phase splitting was performed as illustrated in Fig. 11b, in order to capture the bi-modal nature of the regional porosities and of the amplitude of the velocity field. Regional porosities were as follows, $\varepsilon_\gamma \approx 0.61$ and $\varepsilon_\beta \approx 0.23$. For flow calculations, we used a mesh of approximately 420 000 cells (refined close to the beads wall). Top and bottom boundaries of the cuboid were treated as walls ($\mathbf{v} = 0$), while the lateral faces were periodic.

6.2. Calculation of the velocity field in the periodic unit-cell

To evaluate the velocity field within the representative unit-cell, we impose a macroscopic pressure gradient by introducing a source

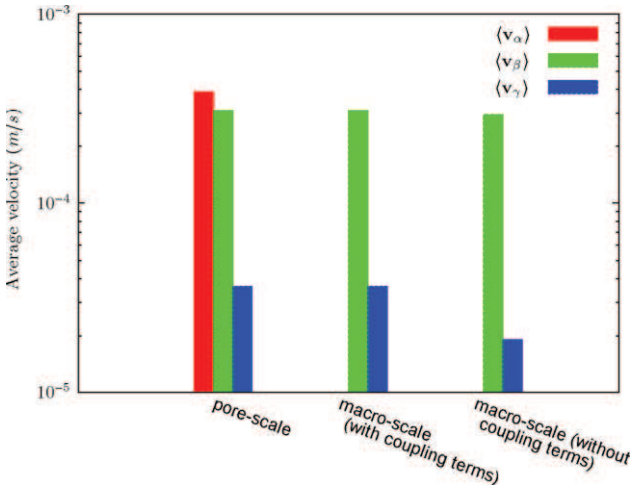

Fig. 13. Comparison of average velocities for the microscale and macroscale simulations, with and without the coupling terms. Pore-scale and complete macroscale results are in very good agreement whereas simulations without the coupling terms yield an error of up to 48%.

term $((\Delta P/L)\mathbf{e}_0)$ into the momentum equation of the Stokes problem (gravity neglected). The unit vector $\mathbf{e}_0$ fixes the orientation while $\Delta P/L$ corresponds to its magnitude. Fluid flow is assumed to be incompressible and at steady-state. The problem was solved using the SIMPLE pressure–velocity coupling procedure proposed by Patankar (1980) with a convergence criterion residuals $\leq 10^{-8}$. Parameters were as follows: $\mathbf{e}_0 = \mathbf{e}_x$, $\Delta P/L = 1$ Pa/m, $\rho = 1000$ kg/m^3 and $\mu = 10^{-2}$ kg/m/s^2. We further remark that this set of parameters implies a creeping flow regime.

The magnitude of the velocity fields, plotted for cross sections in Fig. 12, was in the range $[0, 1.22 \times 10^{-3}$ m/s]. Further, we remark that the distribution exhibits a bi-modal distribution, with relatively large amplitudes (Fig. 12b) in the top layer and an order of magnitude smaller amplitudes in the bottom layer (Fig. 12c). Averaging the velocity field yields, the following regional velocities $\langle v_{\beta_x} \rangle = 3.65 \times 10^{-5}$ m/s and $\langle v_{\gamma_x} \rangle = 3.10 \times 10^{-4}$ m/s, while the Darcy velocity is equal to $\langle v_{\alpha_x} \rangle = 3.47 \times 10^{-4}$ m/s, i.e., closer to the value of the "rapid" region.

6.3. *Effective parameters and macro-scale model*

To compare the results of the microscale simulation against those of the two-pressure model, we first calculated the effective parameters by solving the closure Problems I′–III′ provided in Appendix B. Procedures described in Section 5 were used to obtain $\Pi^*_{\beta_x} = -\Pi^*_{\gamma_x} = -2.4 \times 10^{-9}$ m^{2}s/kg, $h = 1.63 \times 10^{-2}$, $\mathsf{K}^*_{\beta\beta_{xx}} = 1.92 \times 10^{-7}$ m^2, $\mathsf{K}^*_{\gamma\gamma_{xx}} = 2.94 \times 10^{-6}$ m^2, and $\mathsf{K}^*_{\beta\gamma_{xx}} = \mathsf{K}^*_{\gamma\beta_{xx}} = 1.74 \times 10^{-7}$ m^2. We remark that the coupling terms $\mathbf{K}^*_{\gamma\beta}$ and $\mathbf{K}^*_{\beta\gamma}$ are, this time, of the same order of magnitude as $\mathbf{K}^*_{\beta\beta}$ and, therefore, cannot be neglected.

The macroscale geometry consists in a 1D segment, 1 m long. We consider uniform Dirichlet pressure boundary conditions for both the γ and β regions ($p_{\beta_{inlet}} = p_{\gamma_{inlet}} = p_{inlet} = 1$ Pa, $p_{\beta_{outlet}} = p_{\gamma_{outlet}} = 0$ Pa). We can easily show that, at steady-state

$$p_\beta(x) = p_\gamma(x) = \frac{\Delta P}{L}x + p_{inlet} \quad \texttt{with } \Delta P = p_{outlet} - p_{inlet} \tag{129}$$

are solutions of the macroscale problem made of Eqs. (123) and (124) in 1D and the above mentioned Dirichlet boundary condition. Consequently, from Eqs. (111) and (112), one deduces that the regional velocities are constant in the whole 1D domain and are, respectively, equal to

$$\langle v_{\beta_x} \rangle = -\frac{(K_{\beta\beta_x} + K_{\beta\gamma_x})}{\mu}\frac{\Delta P}{L}, \tag{130}$$

$$\langle v_{\gamma_x} \rangle = -\frac{(K_{\gamma\beta_x} + K_{\gamma\gamma_x})}{\mu}\frac{\Delta P}{L}. \tag{131}$$

The histogram (Fig. 13) shows good agreement between the average velocities calculated from the cyclic microscale simulation and those estimated through the analytical macroscopic law equations (130) and (131) (less than 0.1% relative error). Further, in order to emphasize the role played by the coupling terms, we also calculated average velocities from Eqs. (130) and (131) in which $\mathbf{K}^*_{\gamma\beta}$ and $\mathbf{K}^*_{\beta\gamma}$ were neglected. Results are presented in Fig. 13 and show that the average velocities of the γ and β regions are this time underestimated by 5.5% and 48%, respectively.

7. Conclusion

In this paper, we have used the method of volume averaging to derive a macroscale model for the flow of a slightly compressible fluid within bi-structured porous media. The result of this procedure is a two-pressure equation model involving several permeability tensors, a mass exchange coefficient and additional convective transport terms entirely determined by three closure problems to be solved over unit cells representative of the *pore-scale* problem.

If applied to a system that can be dealt with through the two-step upscaling procedure sketched in Fig. 1, the results of this paper provide a solid theoretical basis for a generalization of the model that was derived empirically in Barenblatt et al. (1960) for the flow of a fluid in heterogeneous porous media, and is also coherent with the developments performed in Quintard and Whitaker (1996) for the large-scale homogenization of Darcy's law in heterogeneous media. However, the initial starting points are different: Darcy's law in dual porous media on one side, Stokes equations in our case. As a consequence, the calculation of the effective parameters such as the regional permeabilities and the mass exchange term are performed in a different way. The proposed theory can also deal with dual-media that do not fit in the two-step framework (Fig. 1), hence the introduced concept of bi-structured media. Indeed, the theoretical developments and models were successfully compared to pore-scale direct numerical simulations in the case of a simplified particle filter geometry, which typically does not correspond to a traditional dual-medium (i.e., Fig. 1).

Future work will focus on unsaturated flow in bi-structured porous media. Such an extension of the present theory will supply a solid background to simulate gas–liquid flow in structured packings. Other transport mechanisms may also be investigated, such as mass or thermal dispersion, etc. All the associated macroscale models will involve regional velocities that might be provided by the theory presented in this paper.

Nomenclature

$\langle \cdot \rangle^i$	intrinsic average for the i-phase
$\langle \cdot \rangle$	superficial average
ε_i	volume fraction of the i-phase
V	volume defining the unit-cell (m^3)
V_i	volume of the i-phase within the unit-cell (m^3)
$\mathcal{A}_i$	interfacial area in contact with the i-phase (m^2)
$\mathcal{A}_{i\sigma}$	interfacial area between the i-phase and the solid phase (m^2)
$\mathcal{A}_{\beta\gamma}$	interfacial area between the two ficticious phases (m^2)

ρ_i	density in the i-phase (kg/m^3)
ρ^0	reference density (kg/m^3)
c	compressibility coefficient
$\mathbf{g}$	gravitational acceleration (m/s^2)
$\mathbf{v}_i$	Velocity of the i-phase (m/s)
p_i	pressure field of the i-phase (kg/m/s^2)
P_i	hydrostatic pressure field within the i-phase (kg/m/s^2)
p^0	reference pressure (kg/m/s^2)
μ, μ_i	fluid viscosity (kg/m/s)
l_i	characteristic length of the pore-scale (m)
L	characteristic length of the macro-scale (m)
$\mathbf{r}_i$	position vector (m)
$\mathbf{A}_{ij}$, $\mathbf{A}^0_{ij}$, $\mathbf{B}^1_i$, $\mathbf{B}^2_i$	closure variables (second order tensor)
$\mathbf{a}_{ij}$, $\mathbf{a}^0_{ij}$, $\mathbf{B}^0_i$, $\mathbf{b}^1_i$, $\mathbf{b}^2_i$	closure variables (first order tensor)
b_i	closure variables (scalar)
$\mathbf{K}_i$	permeability tensor (m^2)
$\mathbf{K}_{ij}$	viscous drag tensor (m^2)
$\mathbf{K}^*_{ij}$	multi-domain permeability tensor (m^2)
h, h^*	mass exchange coefficient
$\dot{m}$	mass exchange rate (kg/m^3/s)
$\chi^*_{ij}, \mathbf{\Pi}_i, \mathbf{\Pi}^*_i$	velocity-like coefficient (m/s)
χ_{ij}	effective parameter (m^{-1})

Acknowledgments

This work was fully supported by a research grant from Air Liquide. The participation of Y. Davit was done while he was at OCAMM with support from King Abdullah University of Science and Technology.

Appendix A. Simplifications of the closure problems: one-pressure model

In this appendix, we provide a simplified version of the closure problems, which is more adapted to numerical computations. Our goal is to eliminate the integrals and obtain a purely local form of the boundary value problems. To this end, we use the following decompositions:

$$\mathbf{a}_\alpha = -\mathbf{a}^0_\alpha \cdot \varepsilon_\alpha^{-1} \mathbf{K}_\alpha^{-1}, \tag{A.1}$$

$$\mathbf{A}_\alpha = -\mathbf{A}^0_\alpha \cdot \varepsilon_\alpha^{-1} \mathbf{K}_\alpha^{-1} + \mathbf{I}, \tag{A.2}$$

which, once substituted into Eqs. (42)–(44), yield

$$\nabla \cdot \mathbf{A}^0_\alpha = 0 \quad \text{in } V_\alpha, \tag{A.3}$$

and

$$0 = -\nabla \mathbf{a}^0_\alpha + \nabla^2 \mathbf{A}^0_\alpha + \mathbf{I} \quad \text{in } V_\alpha, \tag{A.4}$$

with

$$\mathbf{A}^0_\alpha = 0 \quad \text{at } \mathcal{A}_{\alpha\sigma}. \tag{A.5}$$

In addition, since porous media are assumed to be cyclic, we have the following periodicity conditions:

$$\mathbf{A}^0_\alpha(\mathbf{r} + \mathbf{l}_k) = \mathbf{A}^0_\alpha(\mathbf{r}) \quad \text{and} \quad \mathbf{a}^0_\alpha(\mathbf{r} + \mathbf{l}_k) = \mathbf{a}^0_\alpha(\mathbf{r}) \quad \text{with } k = 1,2,3. \tag{A.6}$$

To ensure uniqueness of solutions, we have the solvability condition

$$\langle \mathbf{a}^0_\alpha \rangle = 0. \tag{A.7}$$

The permeability tensor, $\mathbf{K}_\alpha$, can be calculated using the relationship $\mathbf{K}_\alpha = \langle \mathbf{A}^0_\alpha \rangle$.

Appendix B. Simplifications of the closure problems: two-pressure model

In this appendix, we present a methodology to determine the effective parameters of the two-pressure model ($\mathbf{K}^*_{ij}$, h and $\mathbf{\Pi}_i$) in the case of the simplified mass exchange rate given by Eq. (122). The continuity equations in Problems I and II become divergence free and we remark that these closure problems are equivalent to those derived in Whitaker (1986a, 1994) or Lasseux et al. (1996) for the classical two-phase flow problem (with a slight difference for the boundary conditions on $A_{\beta\gamma}$). Indeed, in their works they use the general continuity of the normal stress tensor at the fluid–fluid interface that can be expressed as

$$\begin{aligned} &-\mathbf{n}_{\beta\gamma} p_\beta + \mathbf{n}_{\beta\gamma} \cdot \mu_\beta (\nabla \mathbf{v}_\beta + \nabla^T \mathbf{v}_\beta) = -\mathbf{n}_{\beta\gamma} p_\gamma \\ &+\mathbf{n}_{\beta\gamma} \cdot \mu_\gamma (\nabla \mathbf{v}_\gamma + \nabla^T \mathbf{v}_\gamma) + 2\sigma H \mathbf{n}_{\beta\gamma} \quad \text{on } \mathcal{A}_{\beta\gamma}, \end{aligned} \tag{B.1}$$

where $\mathbf{n}_{\beta\gamma}$ is the normal unit vector pointing from β to γ; σ is the surface tension; and H is the curvature. In this paper, we have considered continuity of pressure (see Eq. (8)) at the fluid–fluid interface, so that conditions on the shear stress and surface tension have disappeared.

B.1. Mapping onto $\langle \mathbf{v}_\beta \rangle^\beta$ and $\langle \mathbf{v}_\gamma \rangle^\gamma$

Problems I and II are analogous to those derived by Whitaker (1994). They can be obtained by the following change of variables:

$$\mathbf{A}_{\alpha\beta} = -\mathbf{I}\delta_{\alpha\beta} - \varepsilon_\beta [\mathbf{A}^0_{\alpha\beta} \cdot \mathbf{K}_\beta^{-1} - \mathbf{A}^0_{\alpha\gamma} \cdot (\mathbf{K}_\gamma^{-1} \cdot \mathbf{K}_{\gamma\beta})]; \quad \alpha = \beta, \gamma, \tag{B.2}$$

$$\mathbf{a}_{\alpha\beta} = -\varepsilon_\beta [\mathbf{a}^0_{\alpha\beta} \cdot \mathbf{K}_\beta^{-1} - \mathbf{a}^0_{\alpha\gamma} \cdot (\mathbf{K}_\gamma^{-1} \cdot \mathbf{K}_{\gamma\beta})]; \quad \alpha = \beta, \gamma, \tag{B.3}$$

$$\mathbf{A}_{\alpha\gamma} = -\mathbf{I}\delta_{\alpha\gamma} - \varepsilon_\gamma [\mathbf{A}^0_{\alpha\gamma} \cdot \mathbf{K}_\gamma^{-1} - \mathbf{A}^0_{\alpha\beta} \cdot (\mathbf{K}_\beta^{-1} \cdot \mathbf{K}_{\beta\gamma})]; \quad \alpha = \beta, \gamma, \tag{B.4}$$

and

$$\mathbf{a}_{\alpha\gamma} = -\varepsilon_\gamma [\mathbf{a}^0_{\alpha\gamma} \cdot \mathbf{K}_\gamma^{-1} - \mathbf{a}^0_{\alpha\beta} \cdot (\mathbf{K}_\beta^{-1} \cdot \mathbf{K}_{\alpha\gamma})]; \quad \alpha = \beta, \gamma. \tag{B.5}$$

With similar considerations, one can show, following the developments of Lasseux et al. (1996), that $\mathbf{K}^*_{\gamma\beta}$, $\mathbf{K}^*_{\beta\gamma}$, $\mathbf{K}^*_{\gamma\gamma}$ and $\mathbf{K}^*_{\beta\beta}$ may be evaluated by solving the two following problems:

Problem I'

$$0 = -\nabla \mathbf{a}^0_{i\beta} + \nabla^2 \mathbf{A}^0_{i\beta} - \delta_{\beta i}\mathbf{I} \quad \text{in } V_i; \quad i = \beta, \gamma, \tag{B.6}$$

$$\nabla \cdot \mathbf{A}^0_{i\beta} = 0 \quad \text{in } V_i; \quad i = \beta, \gamma, \tag{B.7}$$

with boundary conditions

$$\mathbf{A}^0_{i\beta} = 0 \quad \text{at } \mathcal{A}_{i\sigma}; \quad i = \beta, \gamma, \tag{B.8}$$

$$\mathbf{A}^0_{\beta\beta} = \mathbf{A}^0_{\gamma\beta} \quad \text{at } \mathcal{A}_{\beta\gamma}, \tag{B.9}$$

$$\mathbf{a}^0_{\beta\beta} = \mathbf{a}^0_{\gamma\beta} \quad \text{at } \mathcal{A}_{\beta\gamma}, \tag{B.10}$$

periodic conditions

$$\mathbf{A}^0_{i\beta}(\mathbf{r} + \mathbf{l}_k) = \mathbf{A}^0_{i\beta}(\mathbf{r}); \quad i = \beta, \gamma; \quad k = 1,2,3, \tag{B.11}$$

$$\mathbf{a}^0_{i\beta}(\mathbf{r} + \mathbf{l}_k) = \mathbf{a}^0_{i\beta}(\mathbf{r}); \quad i = \beta, \gamma; \quad k = 1,2,3, \tag{B.12}$$

and the relationship

$$\langle \mathbf{A}^0_{i\beta} \rangle = -\mathbf{K}^*_{i\beta}; \quad i = \beta, \gamma. \tag{B.13}$$

To ensure uniqueness of the solution, the following constraints have to be satisfied:

$$\langle \mathbf{a}^0_{i\beta}\rangle = 0 \quad \text{with } i=\beta,\gamma. \tag{B.14}$$

Problem II'

$$0 = -\nabla \mathbf{a}^0_{i\gamma} + \nabla^2 \mathbf{A}^0_{i\gamma} - \delta_{\gamma i}\mathbf{I} \quad \text{in } V_i; \quad i=\beta,\gamma, \tag{B.15}$$

$$\nabla\cdot \mathbf{A}^0_{i\gamma} = 0 \quad \text{in } V_i; \quad i=\beta,\gamma, \tag{B.16}$$

with boundary conditions

$$\mathbf{A}^0_{i\gamma} = 0 \quad \text{at } \mathcal{A}_{i\sigma}; \quad i=\beta,\gamma, \tag{B.17}$$

$$\mathbf{A}^0_{\beta\gamma} = \mathbf{A}^0_{\gamma\gamma} \quad \text{at } \mathcal{A}_{\beta\gamma}, \tag{B.18}$$

$$\mathbf{a}^0_{\beta\gamma} = \mathbf{a}^0_{\gamma\gamma} \quad \text{at } \mathcal{A}_{\beta\gamma}, \tag{B.19}$$

periodic conditions

$$\mathbf{A}^0_{i\gamma}(\mathbf{r}+\mathbf{l}_k) = \mathbf{A}^0_{i\gamma}(\mathbf{r}); \quad i=\beta,\gamma; \quad k=1,2,3, \tag{B.20}$$

$$\mathbf{a}^0_{i\gamma}(\mathbf{r}+\mathbf{l}_k) = \mathbf{a}^0_{i\gamma}(\mathbf{r}); \quad i=\beta,\gamma; \quad k=1,2,3, \tag{B.21}$$

and the relationship

$$\langle \mathbf{A}^0_{i\gamma}\rangle = -\mathbf{K}^*_{i\gamma}; \quad i=\beta,\gamma. \tag{B.22}$$

To ensure uniqueness of the solution, the following constraint has to be satisfied:

$$\langle \mathbf{a}^0_{i\gamma}\rangle = 0 \quad \text{with } i=\beta,\gamma. \tag{B.23}$$

B.2. Mapping onto $\langle p_\beta\rangle^\beta - \langle p_\gamma\rangle^\gamma$

We now focus on the treatment of Problem III and the evaluation of h and $\mathbf{\Pi}_i$. We propose the following change of variables:

$$\mathbf{B}_\beta = \mathbf{B}^0_\beta h + \mathbf{B}^1_\beta\cdot(\mathbf{K}^{-1}_\beta\cdot\mathbf{\Pi}_\beta) + \mathbf{B}^2_\beta\cdot(\mathbf{K}^{-1}_\gamma\cdot\mathbf{\Pi}_\gamma), \tag{B.24}$$

$$b_\beta + 1 = b^0_\beta h + \mathbf{b}^1_\beta\cdot(\mathbf{K}^{-1}_\beta\cdot\mathbf{\Pi}_\beta) + \mathbf{b}^2_\beta\cdot(\mathbf{K}^{-1}_\gamma\cdot\mathbf{\Pi}_\gamma), \tag{B.25}$$

$$\mathbf{B}_\gamma = \mathbf{B}^0_\gamma h + \mathbf{B}^1_\gamma\cdot(\mathbf{K}^{-1}_\beta\cdot\mathbf{\Pi}_\beta) + \mathbf{B}^2_\gamma\cdot(\mathbf{K}^{-1}_\gamma\cdot\mathbf{\Pi}_\gamma), \tag{B.26}$$

$$b_\gamma = b^0_\gamma h + \mathbf{b}^1_\gamma\cdot(\mathbf{K}^{-1}_\beta\cdot\mathbf{\Pi}_\beta) + \mathbf{b}^2_\gamma\cdot(\mathbf{K}^{-1}_\gamma\cdot\mathbf{\Pi}_\gamma). \tag{B.27}$$

The closure variables denoted with the superscript "^{0}" correspond to the effects of mass transfer on the deviations problem whereas the ones that wear the superscripts "^{1}" and "^{2}" depict the presence of integrals within the momentum equations. Moreover, in this decomposition b^0_i are scalars, $\mathbf{b}^1_i$, $\mathbf{b}^2_i$ and $\mathbf{B}^0_i$ are first order tensors while $\mathbf{B}^1_i$ and $\mathbf{B}^2_i$ are second order tensors.

It turns out that $(\mathbf{b}^1_i, \mathbf{B}^1_i)$ and $(\mathbf{b}^2_i, \mathbf{B}^2_i)$ satisfy Problems I′ and II′. $(b^0_i, \mathbf{B}^0_i)$ can be evaluated through the following problem:

Problem III'

$$0 = -\nabla b^0_i + \nabla^2 \mathbf{B}^0_i \quad \text{in } V_i; \quad i=\beta,\gamma, \tag{B.28}$$

$$\nabla\cdot\mathbf{B}^0_\beta = \varepsilon^{-1}_\beta \quad \text{in } V_\beta, \tag{B.29}$$

$$\nabla\cdot\mathbf{B}^0_\gamma = -\varepsilon^{-1}_\gamma \quad \text{in } V_\gamma, \tag{B.30}$$

with the boundary conditions

$$\mathbf{B}^0_i = 0 \quad \text{at } \mathcal{A}_{i\sigma}; \quad i=\beta,\gamma, \tag{B.31}$$

$$\mathbf{B}^0_\beta = \mathbf{B}^0_\gamma \quad \text{at } \mathcal{A}_{\beta\gamma}, \tag{B.32}$$

$$b^0_\beta = b^0_\gamma \quad \text{at } \mathcal{A}_{\beta\gamma}, \tag{B.33}$$

and the periodic conditions

$$\mathbf{B}^0_i(\mathbf{r}+\mathbf{l}_k) = \mathbf{B}^0_i(\mathbf{r}); \quad b^0_i(\mathbf{r}+\mathbf{l}_k) = b^0_i(\mathbf{r}); \quad i=\beta,\gamma; \quad k=1,2,3. \tag{B.34}$$

Problems I′, II′ and III′ are linked through the zero average constraints. Consequently, the above closure variables b^0_α, $\mathbf{b}^1_\alpha$ and $\mathbf{b}^2_\alpha$ have to satisfy

$$1 = \langle b^0_\beta\rangle^\beta h + \langle \mathbf{b}^1_\beta\rangle^\beta\cdot(\mathbf{K}^{-1}_\beta\cdot\mathbf{\Pi}_\beta) + \langle \mathbf{b}^2_\beta\rangle^\beta\cdot(\mathbf{K}^{-1}_\gamma\cdot\mathbf{\Pi}_\gamma), \tag{B.35}$$

$$0 = \langle b^0_\gamma\rangle^\gamma h + \langle \mathbf{b}^1_\gamma\rangle^\gamma\cdot(\mathbf{K}^{-1}_\beta\cdot\mathbf{\Pi}_\beta) + \langle \mathbf{b}^2_\gamma\rangle^\gamma\cdot(\mathbf{K}^{-1}_\gamma\cdot\mathit{\Pi}_\gamma). \tag{B.36}$$

To insure uniqueness of the pseudo two-phase flow solution, we must constrain the pressure-like fields in one phase. We choose to impose $\langle \mathbf{b}^1_\beta\rangle^\beta = \mathbf{0}$, $\langle \mathbf{b}^2_\beta\rangle^\beta = \mathbf{0}$ and $\langle b^0_\gamma\rangle^\gamma = 0$. With such conditions, the mass exchange rate h can be directly evaluated through the calculation of the single Problem III' and the following relation:

$$h = \frac{1}{\langle b^0_\beta\rangle^\beta}. \tag{B.37}$$

To obtain $\mathbf{\Pi}^*_i$ we use the equations (B.24) and (B.26) in the zero average relation equation (104). This yields

$$0 = \langle \mathbf{B}^0_\beta\rangle^\beta h + \langle \mathbf{B}^1_\beta\rangle^\beta\cdot(\mathbf{K}^{-1}_\beta\cdot\mathbf{\Pi}_\beta) + \langle \mathbf{B}^2_\beta\rangle^\beta\cdot(\mathbf{K}^{-1}_\gamma\cdot\mathbf{\Pi}_\gamma), \tag{B.38}$$

$$0 = \langle \mathbf{B}^0_\gamma\rangle^\gamma h + \langle \mathbf{B}^1_\gamma\rangle^\gamma\cdot(\mathbf{K}^{-1}_\beta\cdot\mathbf{\Pi}_\beta) + \langle \mathbf{B}^2_\gamma\rangle^\gamma\cdot(\mathbf{K}^{-1}_\gamma\cdot\mathbf{\Pi}_\gamma). \tag{B.39}$$

Since $\mathbf{B}^1_i$ and $\mathbf{B}^2_i$ are solutions of Problems I′ and II′, we obtain

$$\langle \mathbf{B}^1_\beta\rangle = -\mathbf{K}^*_{\beta\beta}; \quad \langle \mathbf{B}^1_\gamma\rangle = -\mathbf{K}^*_{\gamma\beta}; \quad \langle \mathrm{B}^2_\beta\rangle = -\mathbf{K}^*_{\beta\gamma}; \quad \langle \mathrm{B}^1_\gamma\rangle = -\mathbf{K}^*_{\gamma\gamma}. \tag{B.40}$$

According to this remark, Eqs. (B.38) and (B.39) become

$$\mathbf{\Pi}^*_i = h\langle \mathbf{B}^0_i\rangle; \quad i=\beta,\gamma. \tag{B.41}$$

References

Ahmadi, A., Quintard, M., Whitaker, S., 1998. Transport in chemically and mechanically heterogeneous porous media v: two-equation model for solute transport with adsorption. Adv. Water Resour. 22 (1), 59–86.

Barenblatt, G., Zheltov, I., Kochina, I., 1960. Basic concepts in the theory of homogeneous liquids in fissured rocks. J. Appl. Math. (USSR) 24 (5), 1286–1303.

Belfort, G., Davis, R.H., Zydney, A.L., 1994. The behavior of suspensions and macromolecular solutions in crossflow microfiltration. J. Membr. Sci. 96 (1–2), 1–58.

Borsi, I., Lorain, O., 2012. A space-averaged model for hollow fibre membranes filters. Comput. Chem. Eng. 39 (0), 65–74.

Bourbié, T., Coussy, O., Zinszner, B., 1987. Acoustics of porous media. Institut français du pétrole publications.

Brusseau, M., Rao, P., 1990. Modeling solute transport in structured soils: a review. Geoderma 46 (1–3), 169–192.

Cherblanc, F., Ahmadi, A., Quintard, M., 2003. Two-medium description of dispersion in heterogeneous porous media: calculation of macroscopic properties. Water Resour. Res. 39 (6), 1154.

Coats, K., Smith, B., 1964. Dead-end pore volume and dispersion in porous media. Soc. Pet. Eng. J. 4, 73–84.

Gerke, H.H., VanGenuchten, M.T., 1993. A dual-porosity model for simulating the preferential movement of water and solutes in structured porous media. Water Resour. Res. 29, 305–319.

Gray, 1975. A derivation of the equations for multiphase transport. Chem. Eng. Sci. 30, 229–233.

Issa, 1985. Solution of the implicitly discretised fluid flow equations by operator-splitting. J. Comput. Phys. 62, 40–65.

Lasseux, D., Ahmadi, A., Arani, A., 2008. Two-phase inertial flow in homogeneous porous media: a theoretical derivation of a macroscopic model. Transp. Porous Media 75 (December (3)), 371–400.

Lasseux, D., Quintard, M., Whitaker, S., 1996. Determination of permeability tensors for two-phase flow in homogeneous porous media: theory. Transp. Porous Media 24, 107–137.

Mahr, B., Mewes, D., 2008. Two-phase flow in structured packings: modeling and calculation on a macroscopic scale. AIChE J. 54 (3), 614–626.

Oxarango, L., Schmitz, P., Quintard, M., 2004. Laminar flow in channels with wall suction or injection: a new model to study multi-channel filtration systems. Chem. Eng. Sci. 59 (5), 1039–1051.

Patankar, 1980. Numerical Heat Transfer and Fluid Flow. Tay.

Prat, M., 1989. On the boundary conditions at the macroscopic level. Transp. Porous Media 4, 259–280, http://dx.doi.org/10.1007/BF00138039.

Quintard, M., Whitaker, S., 1996. Transport in chemically and mechanically heterogeneous porous media. i: theoretical development of region-averaged equations for slightly compressible single-phase flow. Adv. Water Resour. 19 (1), 29–47.

Quintard, M., Whitaker, S., 1998. Transport in chemically and mechanically heterogeneous porous media iii. large-scale mechanical equilibrium and the regional form of darcy's law. Adv. Water Resour. 21 (7), 617–629.
Skopp, J., Gardner, W., Tyler, E., 1981. Miscible displacement in structured soils: two-region model with small interaction. Soil Sci. Soc. Am. J. 45, 837–842.
Soulaine, C., 2012. Modélisation des écoulements dans les garnissages structurés: de l'échelle du pore à l'céhelle de la colonne. Ph.D. Thesis, Institut National Polytechnique de Toulouse.
Whitaker, S., 1986a. Flow in porous media i: a theoretical derivation of darcy's law. Transp. Porous Media 1, 3–25, http://dx.doi.org/10.1007/BF01036523.
Whitaker, S., 1986b. Flow in porous media ii: The governing equations for immiscible two-phase flow. Transp. Porous Media 1, 105–125.
Whitaker, S., 1987. The role of the volume-averaged temperature in the analysis of non-isothermal, multiphase transport phenomena. Chem. Eng. Comm. 58, 171–183.
Whitaker, S., 1994. The closure problem for two-phase flow in homogeneous porous media. Chem. Eng. Sci. 49 (5), 765–780.
Whitaker, S., 1999. The Method of Volume Averaging. Theory And Applications of Transport in Porous Media, vol. 13. Kluwer Academic Publishers.
Zeman, L., Zydney, A., 1996. Microfiltration and Ultrafiltration: Principles and Applications. Marcel Dekker Inc..